1-1-2017

Underlying Mechanisms Of Arsenic-Induced Tumorigenesis: From Epigenetics To Malignancy

Lingzhi Li
Wayne State University,

UNDERLYING MECHANISMS OF ARSENIC-INDUCED TUMORIGENESIS:
FROM EPIGENETICS TO MALIGNANCY

by

LINGZHI LI

DISSERTATION

Submitted to the Graduate School

of Wayne State University,

Detroit, Michigan

in partial fulfillment of the requirements

for the degree of

DOCTOR OF PHILOSOPHY

2017

MAJOR: PHARMACEUTICAL
SCIENCES (Pharmacology)

Approved By:

_____
Advisor   Date

_____

_____

_____

DEDICATION

I dedicate my dissertation work to my family and friends, for their support and encouragement throughout the process. A special gratitude goes to my mother, Li Li, for giving me her consistent support for the whole five years' doctoral study.

I also dedicate my dissertation work to my friends and lab mates for the support, and especially to our lab manager, Yongju Lu, who has spent a lot of her time helping me out with my project and teaching me the advanced experiments I have never encountered before, and Dr. Xiangmin Zhang for helping me solve the technical problems I came across.

I dedicate my dissertation work to my friends, Dan Luo, Mingyang Zhao, and Huai Huang for being there whenever I have any problem.

ACKNOWLEDGMENTS

I would like to give my special thanks to Wayne State University department of Pharmaceutical Sciences and National Institution of Health for supporting my dissertation work.

I am grateful to my advisor, Professor Fei Chen, as well as my marvelous lab members for their great help and wonderful ideas throughout my studies and research work. I also appreciate my advisor's great guidance and support for my project as well as his insightful comments. In addition, he also helps me a lot for improving my writing skills so that my manuscripts can be published successfully. I also would like to thank my committee members, Dr. Anjaneyulu Kowluru, Dr. David Pitts and Dr. Kezhong Zhang, for their great suggestions and inspiring ideas for my dissertation work.

I would also like to give special thanks to my department for granting me with the opportunity to work with so many wonderful researchers, and also gratitude to Dr. Zhengping Yi's and Dr. Paul Stemmer's groups for their help in the proteomics projects, and Dr. Qingshan Chang for the contributions of the microarray data. Moreover, special thanks to the metabolomics core facility in University of Michigan for their work.

Finally, I would like to thank every individual I mentioned here and elsewhere who have helped me with my dissertation work, for their willingness and support to me all through my doctorate life time.

TABLE OF CONTENTS

v

LIST OF TABLES

LIST OF FIGURES

CHAPTER 1 INTRODUCTION

CHAPTERS CONTAIN MATERIAL FROM PUBLISHED WORK IN WHICH I WAS THE FIRST AUTHOR. THE CO-AUTHORS OF THESE PUBLICATIONS AGREE TO THE USE OF THE PUBLISHED DATA IN THIS DISSERTATION.

1.1 Introduction to Arsenic

Arsenic is a metalloid found in both environmental and occupational settings. In the nature world, arsenic ubiquitously exists in rocks, soil, ground waters, air, food, and in plants and animals in the form of compounds. Naturally, arsenic forms compounds with oxygen, such as oxides (As_2O_3 and As_2O_5), sulfides (As_2S_3 and As_4S_4), as well as compounded with chloride, fluoride, etc. The main source of arsenic exposure in environmental settings is through underground water, contaminated basically with As^{5+} salts, arsenates. According to epidemiological and etiological studies, the prolonged exposure with low dose inorganic arsenic ($>500mg/day\ As^{3+}$) in drinking water is highly associated with several adverse health effects, such as cardiovascular disorders, nervous diseases, diabetes, and also induce renal, hepatic disorders, as well as cancers(Gebel 2000). With respect to occupational settings, inorganic arsenical exposures are documented to chimney sweepers, smelters, sheep-dip workers, and among others (Blejer and Wagner 1976).

There are multifaceted routes for arsenic exposure, from direct ingestion such as drinking and eating, to touching, and even inhalations. For example, welding workers are exposed to welding fumes including inorganic arsenic, and

according to previous reports their lungs and other organs are readily to be damaged because of inhalations of such fumes (Meo and Al-Khlaiwi 2003). Despite of natural arsenicals, there are also artificial synthetic arsenates, such as Paris Green for painting pigment, calcium arsenate, and lead hydrogen arsenate, used as agricultural insecticides, etc., and with such diversity of arsenicals applications the potential for arsenic exposure increases dramatically. Accordingly, an estimation of 160 million people is with the risk of arsenic exposure worldwide only through water (Joseph, Dubey et al. 2015), let alone the whole population of all the pathways for arsenic propagation.

As what had been reported, cells take up arsenic through different membrane transporters, for example, the aquaglyceroporins in human and rat cells (Liu, Carbrey et al. 2004), and hexose permeases in Saccharomyces cerevisiae (Liu, Boles et al. 2004). The penetration of arsenate into the cells could be achieved through some phosphate transporters(Calatayud, Gimeno et al. 2010). After ingestion, arsenic will be metabolized to its methylated forms, monomethyl arsenic acid (MMA) and dimethylarsinic acid (DMA), either compounded with trivalent or pentavalent arsenic. With the most updated information, its organic metabolites are still carcinogenic (Anetor, Wanibuchi et al. 2007), but only after metabolism arsenic could be eliminated from system. Accordingly, the mechanisms underlying arsenic metabolites include DMA's clastogenic effects (Wanibuchi, Salim et al. 2004), MMA's ROS-generating abilities (Nishikawa, Wanibuchi et al. 2002), etc. In general, inorganic arsenic

methylation has been considered as a way to detoxification. However, emerging evidence indicates the carcinogenic effects of its metabolites.

1.2 Arsenic as a carcinogen

The role of arsenic has been widely studied for decades. Based on cell types and its underlying mechanisms, arsenic has been viewed as "Janus-type". On one hand, arsenic had long been considered as an environmental carcinogen. On the other hand, as proposed and practiced originally by the traditional Chinese medicine, arsenic has been used as a chemo-therapeutic agent for acute promyelocytic leukemia (APL). The specific feature of APL is the chromosomal translocation, t (15, 17), yields PML-RARα fusion, and arsenic targets this fusion, leading to cell death consequently (Chou and Dang 2005).

The oncogenic activities of arsenic have been documented for several decades. The International Agency for Research on Cancer (IARC) reported involvement of inorganic arsenic for the increased skin cancer incidence in 1973. Following that, IARC updated arsenic carcinogenicity successively in 1980, 1987, 2004, and 2009(Tokar, Benbrahim-Tallaa et al. 2010), with an expansion to lung, urinary bladder, kidney, liver and prostate cancer. The possible mechanisms underlying arsenic carcinogenicity are manifold. For example, according to our previous studies, arsenic can induce a variety of carcinogenic pathways, including a moderate expression of NF-κB (Chen, Ding et al. 2001), MAPK proliferative pathways (Chen, Liu et al. 2013, Li, Qiu et al. 2014, Sun, Yu et al. 2014), Akt activation (Beezhold, Liu et al. 2011, Liu, Chen et al. 2012, Chen, Liu

et al. 2013, Li, Qiu et al. 2014, Li, Lu et al. 2015), excessive ROS generation (Li, Qiu et al. 2014), as well as regulations of several miRNAs (Beezhold, Castranova et al. 2010, Beezhold, Liu et al. 2011, Chen, Liu et al. 2013, Sun, Yu et al. 2014). Furthermore, our studies also corroborate that arsenic exposure is associated with epigenetic regulations, malignancy control, and cell cycle arrest. In addition, we have previously reported that mineral dust-induced gene (mdig), a suspected histone demethylase, also responds to arsenic treatment (Sun, Yu et al. 2014), leading to changes on the epigenetic landscape of the genome. Overexpression of mdig is oncogenic through increasing cancer cell proliferation. However, mdig might inhibit migration/invasion of the cells derived from lung cancer or breast cancer(Yu, Sun et al. 2014). As for arsenic-induced cell cycle regulations, we have proposed that arsenic post-transcriptionally upregulates GADD45 α, a key regulator for cells checkpoint functions (Zhang, Bhatia et al. 2006, Chang, Bhatia et al. 2007). Additionally, we have also reported that arsenite causes G2/M cell cycle arrest through CDC25C degradation (Chen, Zhang et al. 2002), suggesting arsenic is with potential to interrupt cell cycle progression. Our recent data also indicated a positive association between arsenic exposure and cancer cell stemness (Chang, Chen et al. 2014). Taken together, arsenic elicits its carcinogenic role through regulations on multiple signaling pathways, such as NF-κB, MAPK, Akt, ROS, miRNAs, cell cycle, etc.

1.2.1 Effects of arsenic on NF–κB

NF-κB (nuclear factor kappa-light-chain-enhancer of activated B cells) is a transcription factor that is responsible for up-regulations of inflammatory cytokines, inducible nitric oxide synthesis, superoxide dismutase (MnSOD), anti-apoptotic genes, growth factors and several oncogenes (Karin 2008). The NF-κb family contains five members, including NF-κB1(p50/p105), NF-κB2 (p52/p100), RelA (p65), RelB, and c-Rel(Chen, Demers et al. 2002). At the resting states, NF- κB is inactivated by its inhibitory partners, IκB family members, such as IκBα, IκB β, and IκB ε, in cytoplasm. Once stimulated by arsenic or other stresses, IκB will be phosphorylated by its kinase, IKK (IκB kinase), ubiquitinated and degraded by proteasome, leading to releasing of NF-κB from the association with IκB and translocation of NF-κB to nuclei. A plethora of extracellular stimuli, including bacterial products, viral proteins, some carcinogenic metals, and reactive oxygen species (ROS), can initiate the upstream signaling for the activation of IKK and NF-κB(Li, McGrath et al. 2013).

There is evidence suggesting that arsenic-induced NF-κB activation might be mediated by the excessive generation of ROS (Hu, Jin et al. 2002, Li, Cai et al. 2002, Henkler, Brinkmann et al. 2010) (Fig. 1.1). As summarized in Figure 1.1, arsenic induces excessive generation of ROS from mitochondria and endosomes respectively after being taken up through specific transporters as discussed above. These ROS further activate NF-κB and other transcription factors, such as AP-1 directly (Chowdhury, Chatterjee et al. 2010), or through other nodal molecules. For example, the endosomal ROS foster IL-R1 complex recruitment

on endosomal membranes and further phosphorylates IKK so that NF-κB is activated (Li, Harraz et al. 2006). However, depending on the duration and degree of ROS generation, the oxidative stress induced by ROS may exhibit opposite roles on the NF-κB signaling. There are reports demonstrating that the release of ROS from mitochondria hampers further NF-κB activation because of the extra oxidation on IKK(Kapahi, Takahashi et al. 2000). Without question, NF-κB is a key mediator for the arsenic-induced carcinogenesis and inflammation (Fry, Navasumrit et al. 2007).
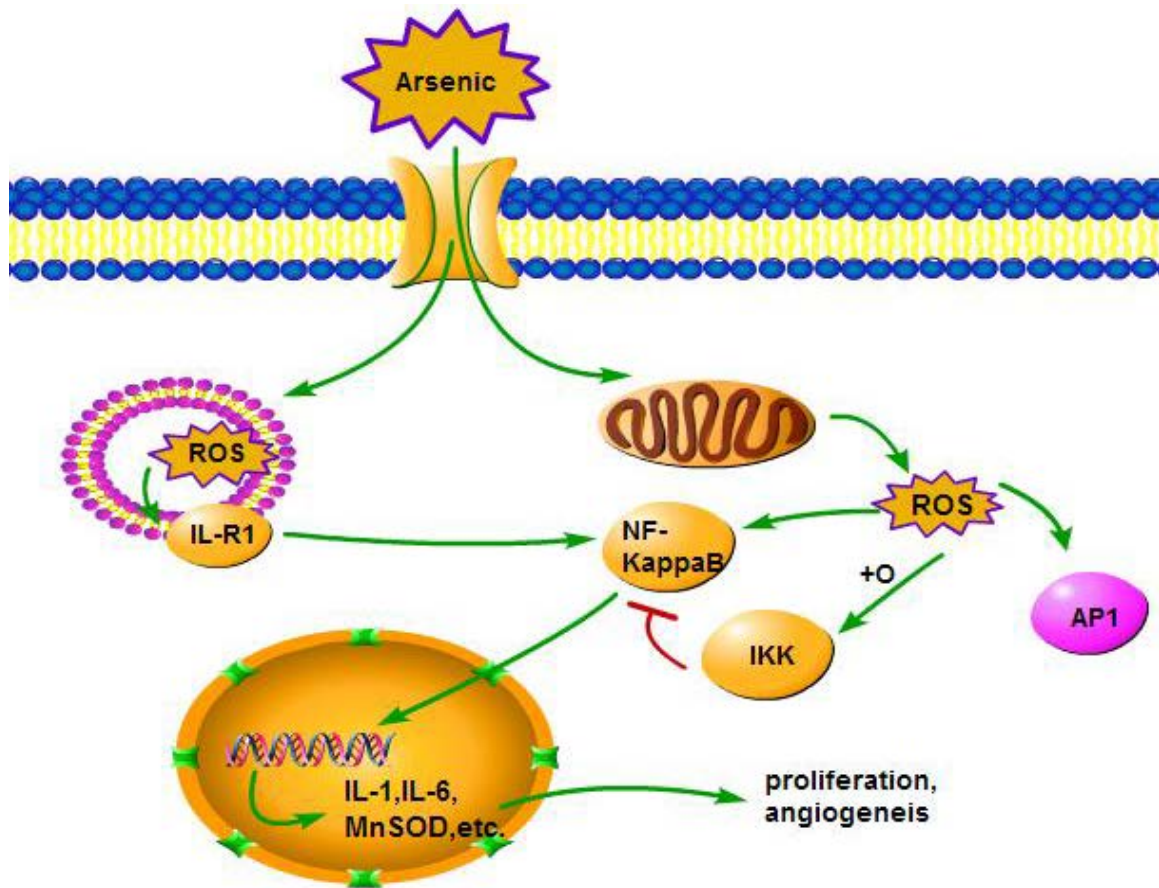
Figure 1.1 Overview of the effects of arsenic on NF-κB regulations.

Extracellular arsenic enters into cells through certain transporters on plasma membrane. The intracellular arsenic undergoes metabolism, and its reactive oxidative metabolites induce the activation of NF-κB and other transcription factors. The activated NF-κB translocates into nucleus to regulate expression of certain genes to sustain cell growth, transformation and angiogenesis.

1.2.2 The role of arsenic-induced oxidative stress in carcinogenesis

As discussed, intracellular arsenic is able to induce oxidative stress. There are several types of Reactive Oxygen Species (ROS) and Reactive Nitrogen

Species (RNS) generated during arsenic metabolism, including hydrogen peroxide (H_2O_2), hydroxyl radical ($HO^•$), superoxide anion ($O_2^{•-}$), Nitric Oxide ($NO^•$), peroxynitrite(Liu and Jan 2000) and some reactive intermediates, such as dimethylarsenic peroxyl radical [$(CH_3)_2AsOO^•$] and dimethylarsinic radical [$(CH_3)_2As^•$] (Del Razo, Quintanilla-Vega et al. 2001).

Extensive studies have been made on the role of ROS on protein modification, lipid oxidation and DNA damage response. An earlier study reported that gavage feeding of mice with 220 mg/kg of DMA (Dimethylarsenate) induced higher levels of ROS that directly damage DNA, which contributes to the further liver carcinogenesis (Wanibuchi, Hori et al. 1997). Furthermore, our previous studies also demonstrated that arsenic promotes expression of GADD45α, a DNA damage response protein, through the accumulation of ROS in the bronchial epithelial cell line, BEAS-2B cells, which supported the notion of ROS-related DNA damage (Bower, Leonard et al. 2006). Meanwhile, there is evidence indicating that oxidative posttranslational modifications of proteins are caused by reactions between free radicals and protein residues(Cai and Yan 2013), leading to the loss of original function of proteins. Collectively, oxidative stress-induced damage on protein, lipid and DNA, and/or the consequent damage responses are important contributors to various types of diseases, such as cancer, hepatitis and among others. Thus, the abnormal ROS generation certainly plays important role of cell transformation and stem cell formation in response to arsenic.

In our recent studies, we had shown unique patterns of ROS generation in the cells subjected to a short-term and long-term treatment with arsenic (Chang, Pan et al. 2010). In a short-term treatment, arsenic was highly capable of inducing ROS generation in the BEAS-2B cells. In contrast, the ROS generation capacity of the cells with long-term arsenic treatment was significantly compromised. Interestingly, the cells following long-term arsenic treatment not only showed features of malignant transformation, but also acquired characteristics of the cancer stem-like cells. The underlying mechanisms of how long-term arsenic treatment reduces ROS generation and such an effect contributes to cancer development are still not fully understood. Nonetheless, we could make certain plausible speculations. One of those may be due to some specific characteristics of the cancer stem-like cells. Several lines of evidence had indicated a general reduction of ROS generation in normal stem cells and assumed that this is an important measure to maintain the stemness and prevent differentiation of the stem cells (Shen, Wang et al. 2015). It is also very likely that increased ROS will trigger the p38 and FoxO3 system that drive differentiation of the stem cells (Sato, Okada et al. 2014). Furthermore, either cancer cells, cancer stem cells, or normal stem cells, relay on the higher rate of aerobic glycolysis (Warburg effect), rather than mitochondrial oxidative phosphorylation that produces ROS, for the generation of energy in order to survive the hypoxia conditions. More relevant details in this regard will be discussed in chapter two.

Nevertheless, overwhelming generation of ROS in normal cells may mediate the carcinogenesis of arsenic through oxidative damage of the DNA, lipids and proteins, or facilitating genetic mutations due to the interference of the repairing processes of the damaged DNA (Fig.1.2).
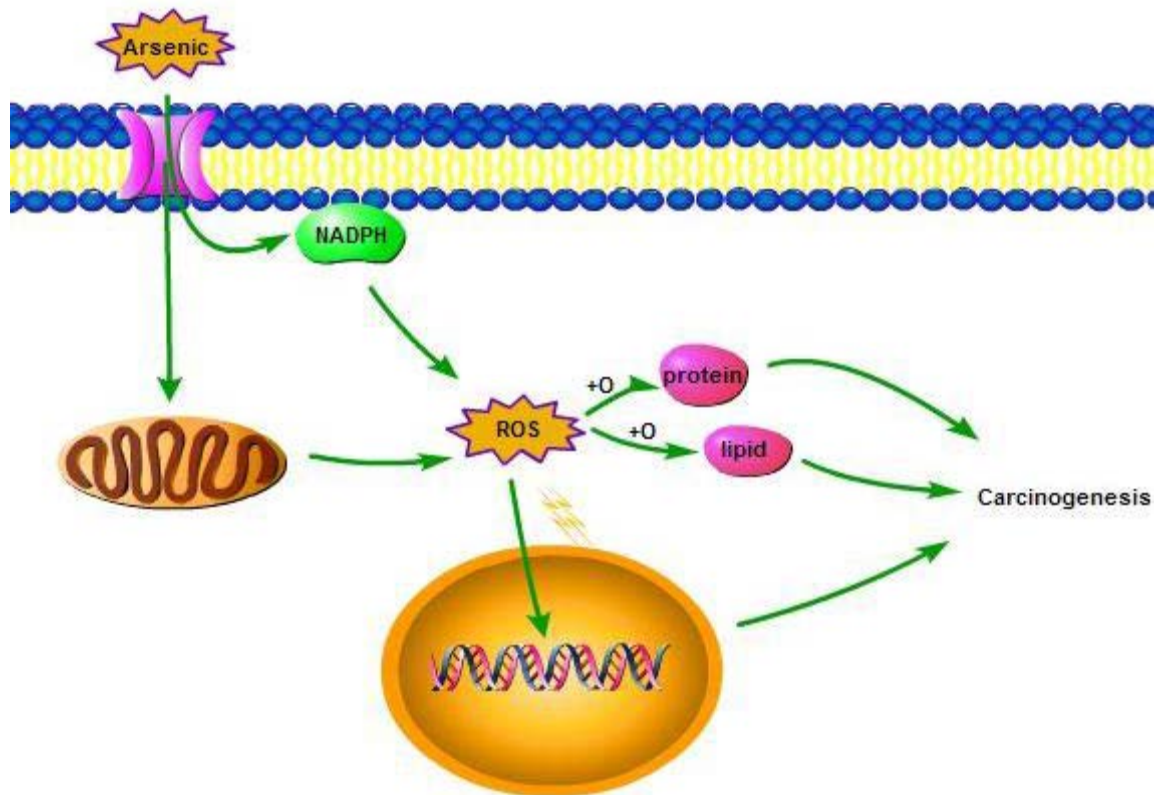
Figure 1.2 Overview of the effects of ROS on arsenic-induced carcinogenesis. Extracellular arsenic gets into cells through certain transporters on plasma membrane. The intracellular arsenic undergoes metabolism, and its reactive oxidative metabolites will cause damage to protein, lipid and DNA. Consequently, the excessive ROS will contribute to arsenic-induced transformation of the normal cells, leading to carcinogenesis.

1.2.3 Arsenic-induced carcinogenesis through Mitogen-Activated Protein Kinase (MAPK) pathway

A plethora of studies have indicated critical roles MAPK in cell proliferation, compensatory growth and malignant transformation of the cells (Chang and Karin 2001). MAPK is activated through the cascade of MAPK kinase kinase (MEKK), MAPK kinase (MEK or MKK) and MAPK, and inactivated by the corresponding protein phosphatases (English, Pearson et al. 1999). In mammalian cells, this group of kinases includes extracellular signal-related kinases (ERK), Jun amino-terminal kinases (JNK), and p38. Each of these kinases had been linked to carcinogen-induced carcinogenesis or tumorigenesis through different or overlapping mechanisms.

In BEAS-2B cells, our previous studies showed that arsenic is able to induce JNK activation and further sustain the expression of Growth arrest– and DNA damage–induced gene 45α (GADD45α)(Chen, Lu et al. 2001). The up-regulated GADD45α acts as a cell cycle regulator and consequently induces G2/M cell cycle arrest. In non-cancerous cells, such as BEAS-2B, cell cycle arrest functions more as a negative regulator for cell growth since such arrest will intervene with normal mitosis and therefore lead the mitotic cells into the quiescent state. On the other hand, for the transformed or cancerous cells it falls into another scenario. For the heavily mutated transformed cells such elevated cell cycle regulators will also arrest the highly mitotic cells into the quiescent state, but at the same time such intervention will provide extra time for those transformed

cells undergoing the error-prone repair processes, hence foster cell survival. In addition to cell cycle regulations, JNK has also been studied with the ability of inducing myc expression stimulated by low dose arsenic treatment, and such increased myc may further contribute to arsenic induced cell malignant transformation(Chang, Chen et al. 2014). Furthermore, JNK activation has also been associated with the phosphorylation and intracellular redistribution of Enhancer of Zeste Homolog 2 (EZH2) (Li, Qiu et al. 2014), which will be discussed in detail in the next chapter.

Other members of the MAPK family may be also involved in the oncogenic effects of arsenic, for example, the accumulated ROS following arsenic exposure are highly capable of promoting ERK activation, therefore, sustain cell proliferation(Chowdhury, Chatterjee et al. 2010, Li, Qiu et al. 2014) and transformation (Dong 2002, Li, Lee et al. 2011). With the respect of p38, we had also showed a ROS-dependent activation of p38 by arsenic (Li, Qiu et al. 2014). Depending on the types of cells and the sub-family members of this kinases, activation of p38 can either be pro-carcinogenic or anti-carcinogenic. When p38α was predominantly activated, a cell cycle arrest at the G1/S or G2/M phase occurs (Namgung and Xia 2001), which may one of the anti-leukemia mechanisms of arsenic. In contrast, if p38δ was activated, the cells were more likely in the proliferative status (Zhong, Lardinois et al. 2011).

In summary, arsenic can regulate the activation of the MAPK family members, possibly through a ROS-dependent mechanism as depicted in Figure

1.3. Concordantly with previous studies on biological functions of MAPKs, it is likely that MAPKs are the key modulators in the signaling cascades for the arsenic-induced cell transformation and carcinogenesis, esp. the JNK kinase. Although the pro-apoptotic effect of JNK activation had been extensively studied and documented, accumulating evidence also suggested pivotal roles of JNK in compensatory growth of the damaged tissues, proliferation of the cancer cells, and the maintenance of the stemness of the stem cells or cancer stem-like cells through the expression of c-myc, Oct4, Sox2, and other self-renewal factors(Chen 2012).
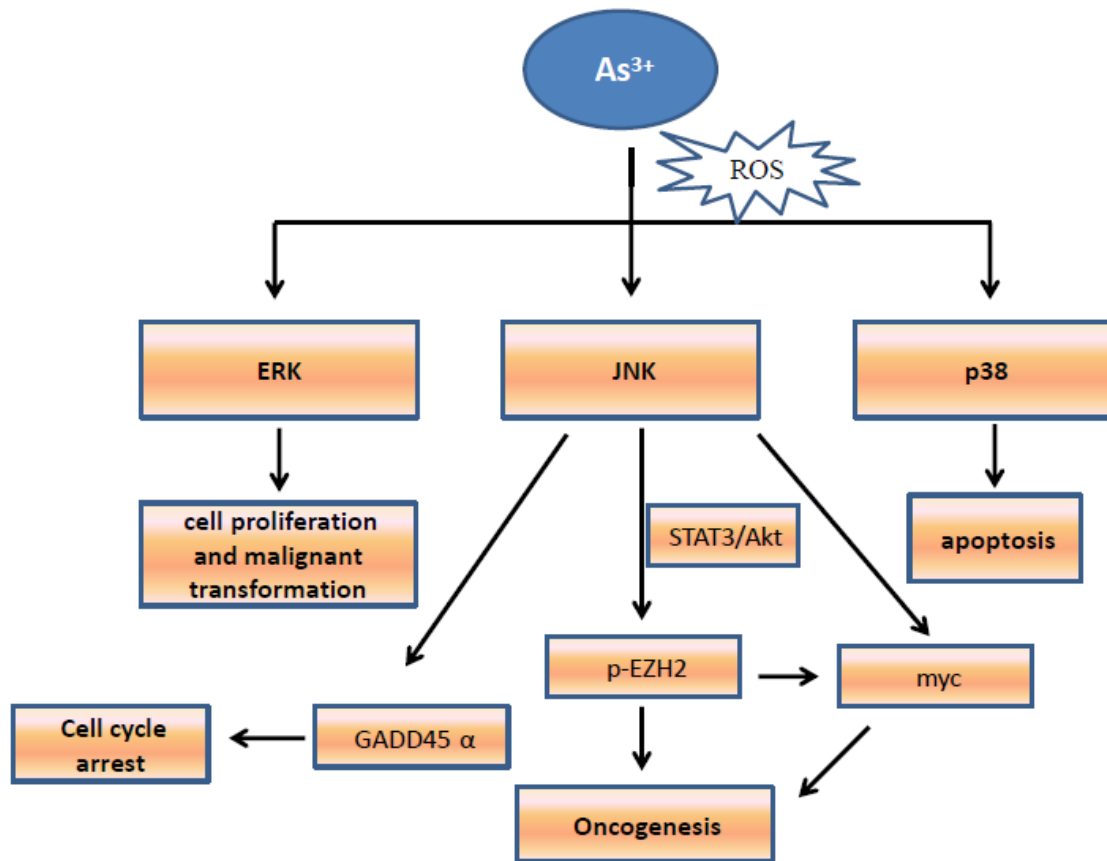
Figure 1.3 Overview of MAPK pathways in arsenic biological functions.

Arsenic exposure will lead to the generation of excessive ROS, and cause oxidative stress of the cells, which leads to activation of the MAPK family members, ERK, JNK and p38. The activated MAPKs will mediate different signaling cascades that play important roles in arsenic-induced carcinogenesis.

CHAPTER 2 EPIGENETIC REGULATIONS OF ARSENIC IN TUMORIGENESIS CHAPTERS CONTAIN MATERIAL FROM PUBLISHED WORK IN WHICH I WAS THE FIRST AUTHOR. THE CO-AUTHORS OF THESE PUBLICATIONS AGREE TO THE USE OF THE PUBLISHED DATA IN THIS DISSERTATION.

2.1 Introduction

Epigenetics refer to the modifications on genomes without changes in DNA sequences. The most typical epigenetic modifications include non-coding RNAs, DNA methylation, and histone tail modifications by acetylation, methylation, phosphorylation, ubiquitination. We had previously provided evidence showing that arsenic induces EZH2 phosphorylation through ROS/JNK/Stat3/Akt signaling cascade. EZH2 is a methyltransferase subunit in the PRC2 complex responsible for the tri-methylation of lysine 27 on histone H3 (H3K27me3). There is a report suggested that phosphorylated EZH2 might methylate Stat3, leading to a sustained Stat3 activation to maintain the stemness of glioblastoma stem cells (Kim, Kim et al. 2013). Thus, our studies on the arsenic-induced EZH2 phosphorylation may unravel an additional mechanism on the carcinogenesis or tumorigenesis resulted from environmental arsenic exposure. In our preliminary studies, we had provided experimental evidence suggesting that phosphorylated EZH2 is able to interact with the cap-independent translation machinery, the internal ribosome entry site (IRES) complex to initiate protein translation of c-myc, a well-documented oncogene. Furthermore, we have also tested the role of some small non-coding RNAs, mostly miRNAs, in the arsenic-induced malignant

transformation from the aspects of energy metabolic reprogramming. Given the fact that altered metabolism is considered as a new hallmark of cancer process(Hanahan and Weinberg 2011), understanding how arsenic promotes metabolic reprogramming will yield new insights into the molecular mechanisms and molecular targeting of cancers.

2.2 EZH2 phosphorylation and intracellular redistribution during arsenic-induced malignant transformation of the cells.

Arsenic had been reported to regulate proteins that modify histone tails, and contribute to carcinogenesis (Roy, Son et al. 2015). In our previous studies, we have demonstrated that arsenic promotes EZH2 phosphorylation at Serine21 through JNK/Stat3/Akt signaling pathway (Chen, Liu et al. 2013). However, the biological significance of this signaling remain to be fully understood. It has been reported that majority of EZH2 proteins are associated the SUZ12, EED, and RbAp46.48 to form polycomb repressive complex 2 (PRC2) that transfers 3 methyl groups to H3K27, and yields gene silencing. Recently, emerging evidence also indicates other components of PRC2, such as AEBP2, PCLs and JARID2 (Roy, Son et al. 2015). In addition to EZH2, EZH1 that plays a similar enzymatic role on H3K27 methylation, can also be incorporated into the PRC2 complex. Nevertheless, some subtle differences between EZH2 and EZH1 exist. For example, EZH1 could be found in the cells in regardless of the proliferative status, whereas EZH2 most likely expressed in the highly proliferative cells (Margueron, Li et al. 2008). Accordingly, it is not surprising to note an increased

expression of EZH2 in various types of cancers (Hock 2012). Meanwhile, mounting evidence indicates the fact of arsenic-induced mitochondrial dysfunction (Zheng, Lam et al. 2015), resulting in the generation of excessive ROS (Reactive Oxygen Species), and the accumulated ROS are highly involved in the tumorigenesis process(Prasad, Gupta et al. 2017). Thus, we hypothesize that arsenic-induced EZH2 phosphorylation and translocation from nucleus to cytoplasm is achieved through ROS/JNK/Stat3/Akt signaling pathway during arsenic-induced carcinogenesis.

In agreement with our earlier report, we observed that arsenic (As^{3+}) is able to induce serine 21 (S21) phosphorylation of the EZH2 in human bronchial epithelial cell line, BESA-2B cells (Fig. 2.2.1A). To determine the involvement of oxidative stress resulted from ROS generation in this As^{3+}-induced EZH2 phosphorylation, we pre-treated the cells with 20 mM N-acetyl-L-cysteine (NAC), a general antioxidant that provides the cells with sufficient amount of glutathione to minimize the oxidation of cellular proteins, lipids, and DNA (Sadowska et al., 2006), for 2h and then treated the cells with 20 μM As^{3+} for 1,2, or 4 h. A significant reduction in EZH2 phosphorylation was noted in the cells treated with NAC (Fig. 2.2.1A). NAC is also capable of inhibiting As^{3+}-induced activation of Akt, STAT3, and JNK (Fig. 2B and C), the upstream kinases associated with the S21 phosphorylation of the EZH2. In addition, NAC is also potent in diminishing the As^{3+}-induced activation of ERK and p38 (Fig. 2.2.1D), two mitogen-activated protein kinases that respond to the oxidative stress. To validate the contribution

of ROS in As^{3+}-induced S21 phosphorylation of the EZH2, we also tested the capability of H_2O_2, one of the most abundant and important ROS, on EZH2 phosphorylation and kinase activation. Indeed, an earlier occurrence of S21 phosphorylation of the EZH2 was noted in the cells treated with 0.2mM H_2O_2 for 5 to 15 min (Fig. 2.2.1E), which correlates with the time-dependent activation of Akt and the dose-dependent Akt activation in the cells treated with different concentrations of H_2O_2 for 5 min (Figs. 2.2.1E and F).
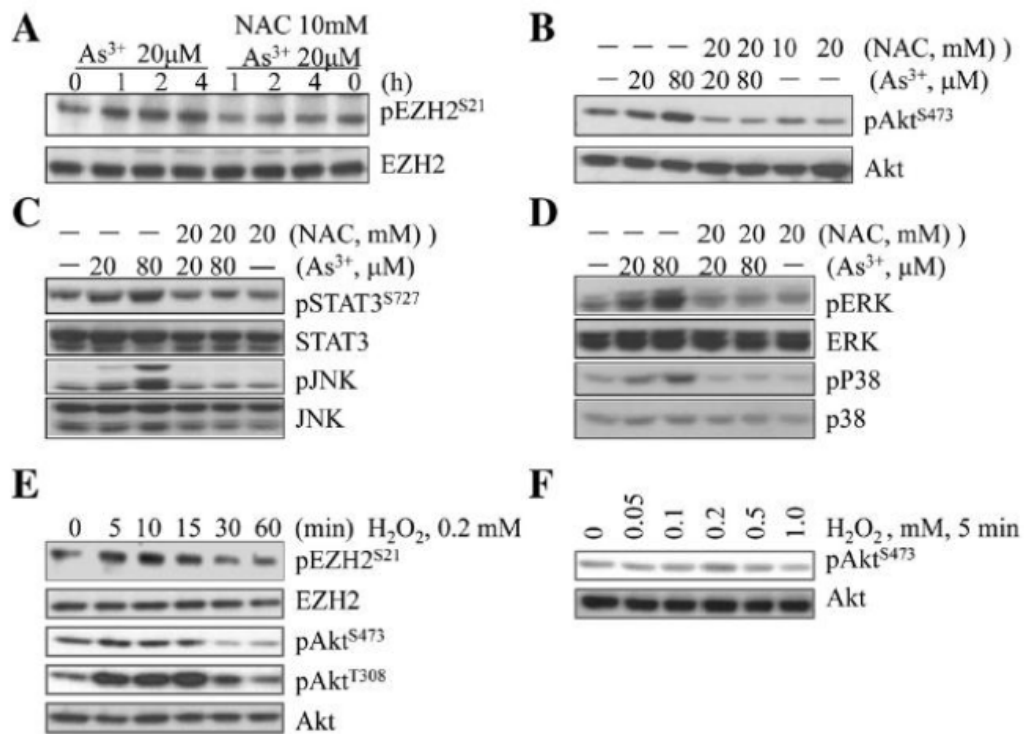
Figure 2.2.1 Involvement of oxidative stress in As^{3+}-induced kinase activation and EZH2 phosphorylation in BEAS-2B cells.

(A) BEAS-2B cells were treated with 20 μM As^{3+} for 0, 1, 2, or 4 h with or without NAC pretreatment for 2 h. S21 phosphorylation of the EZH2 ($pEZH2^{S21}$) protein

was determined by Western blotting. The most right lanes (0 h As^{3+}) are NAC only treatment. (B–D) The activation of Akt (B), STAT3 and JNK (C), and Erk and p38 (D) were determined in the BEAS-2B cells treated with 20 or 80 μM As^{3+} for 2 h in the presence or absence of NAC pretreatment for 2 h. In each panel, the most right lanes (without As^{3+}, —) are NAC only groups. (E) H_2O_2 induces $pEZH2^{S21}$ and Akt activation in a time-dependent manner. (F) Dose-dependent activation of Akt kinase in the BEAS-2B cells treated with the indicated concentrations of H_2O_2 for 5 min.

To explore whether the above observations are cell type specific or not, we extended this study in other type of cells too. A549 is a cell line derived from the non-small cell lung cancer (NSCLC) with some features of alveolar type II cells. The S21 phosphorylation of the EZH2 could be observed in the A549 cells treated with 20 μM As^{3+} for 1 to 4 h with a peak phosphorylation at 2 h, which is roughly parallel with the pattern of Akt activation by As^{3+} (Fig. 2.2.2A). A significant decrease of both EZH2 phosphorylation and Akt activation in response to As^{3+} was noted in the cells pre-treated with 10 or 20 mM NAC (Fig. 2.2.1A), indicating that oxidative stress due to ROS induction by As^{3+} is also involved in the S21 phosphorylation of the EZH2 protein in A549 cells. To address this notion further, the A549 cells were treated with different concentrations of H_2O_2 for 5 min or 500 μM H_2O_2 for 5 to 60 min. As depicted in Fig. 2.2.2B, H_2O_2 is capable to induce S21 phosphorylation of the EZH2 along with the activation of the upstream kinases, including JNK, STAT3, and Akt. To extend above

observations, we also tested the inducibility of EZH2 phosphorylation by As^{3+} at much lower concentrations from 0.25 to 4 µM in the cells cultured for a prolonged time, 72 h. We noted that lower concentrations of As^{3+} was able to induce JNK and p38 activation in a clear dose-dependent manner (Fig. 2.2.2C and data not shown). However, a significant Akt activation by lower concentrations of As^{3+} could not be detected (top two panels, Fig. 2.2.2C). The treatment of the cells with 0.25 or 2 µm As^{3+}-induced S21 phosphorylation of EZH2 (Fig. 2.2.2D). Unexpectedly, NAC appeared to be unable to inhibit the EZH2 phosphorylation induced by As^{3+} at lower concentrations. In other experiments, we demonstrated that prolonged incubation of the cells with NAC, e.g., 72 h, enhanced both basal and As^{3+}-induced p38 activation, possibly because of stress responses due to the overwhelmed reduction condition. Accordingly, we speculate that different mechanisms may be involved in the EZH2 phosphorylation induced by low and high concentrations of As^{3+}, respectively.
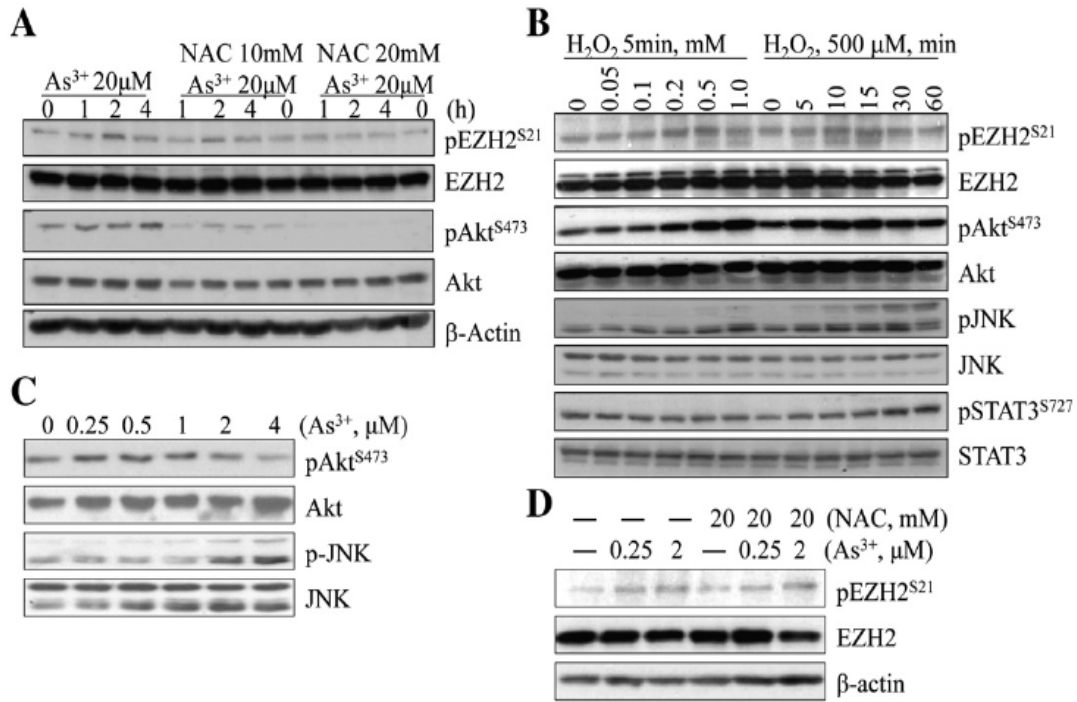
Figure 2.2.2 Oxidative stress contributes to As^{3+}-induced EZH2 phosphorylation and kinase activation in A549 cells

(A) A549 cells were treated with 20 µM As^{3+} for the indicated time with or without NAC pretreatment for 2 h. The levels of pEZH2^{S21} and Akt activation were determined by Western blotting. The NAC only groups were indicated as 0 h As^{3+} treatment. (B) Dose- and time-dependent EZH2 phosphorylation and kinases activation in A549 cells treated with H_2O_2. (C) Lower concentrations of As^{3+} induce JNK but not Akt activation in the A549 cells treated with As^{3+} for 72 h. (D) NAC was unable to inhibit lower concentration As^{3+}-induced EZH2 phosphorylation in the cells cultured for 72 h.

In BEAS-2B cells, we had previously shown the cytoplasmic translocation of the S21-phosphorylated endogenous EZH2 from nuclei in response to As^{3+} treatment (Chen et al., 2013). To investigate if As^{3+} is able to induce the same translocation of the exogenous EZH2, the BEAS-2B cells expressing GFP-EZH2 were treated with 20 μM As^{3+} for 2 h. The GFP-EZH2 is exclusively localized in the nuclei of the cells without As^{3+} treatment (Fig. 2.2.3 A, upper panels). Following As^{3+} treatment, both cytoplasmic and nuclear locations of the GFP-EZH2 were observed (Fig. 2.2.3 A, bottom panels). Furthermore, As^{3+} appeared to be able to induce the clustering of GFP-EZH2 proteins. These clusters were randomly distributed in both cytoplasm and nucleus. To explore whether oxidative stress is involved in As^{3+}-induced re-distribution of the GFP-EZH2, NAC was applied prior to As^{3+} treatment. As shown in Fig. 2.2.3 B, NAC prevented the cytoplasmic localization of the GFP-EZH2 induced by either 20 μM or 80 μM As^{3+}, indicating that the oxidative stress is involved in As^{3+}-induced cytoplasmic localization of the EZH2 protein. However, NAC was unable to prevent the nuclear clustering of the exogenous GFP-EZH2 proteins induced by As^{3+}. The possible role of oxidative stress on the intracellular distribution of the EZH2 protein was confirmed by the treatment of the cells with 0.2 mM H_2O_2 that clearly induced cytoplasmic localization of the GFP-EZH2 proteins (Fig. 2.2.3 B, bottom panels). Semi-quantification suggested a more than 50% inhibition of the As^{3+}-induced cytoplasmic localization of the exogenous EZH2 (GFP-EZH2) by NAC (Fig. 2.2.3 C). To further confirm the effect of As^{3+} and/or oxidative stress

on the cytoplasmic localization of the EZH2 proteins, we fractionated the cell lysates by isolating cytoplasmic and nuclear fractions, respectively, followed by measuring the levels of S21-phosphorylated and the total endogenous EZH2 proteins in response to As^{3+} or H_2O_2 treatment. Although As^{3+} appeared to be unable to affect the nuclear levels of the phosphorylated EZH2 (pEZH2) and EZH2, As^{3+} was able to increase both pEZH2 and EZH2 in the cytoplasmic fraction (Fig. 2.2.4 A). The pretreatment of the cells with 20 mM NAC reduced As^{3+}-induced pEZH2 in the cytoplasmic fraction significantly. NAC was also able to reduce the level of total EZH2 in the cytoplasmic fraction, although with a lesser extent relative to its effect on the phosphorylated EZH2.
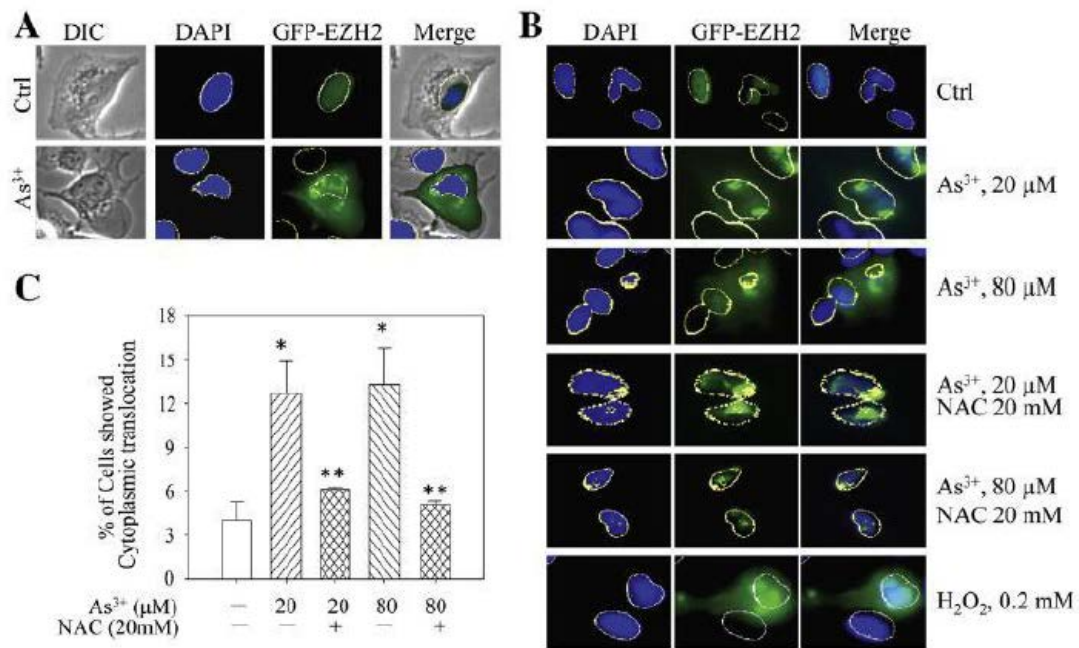
Figure 2.2.2 Both As^{3+} and H$_2$O$_2$ induce cytoplasmic localization of the EZH2 protein in BEAS-2B cells.

(A) BEAS-2B cells expressing GFP-EZH2 were treated with 20 μM As^{3+} for 2 h. The intracellular distribution of EZH2 was determined by immunofluorescent microscopy. (B) NAC prevented cytoplasmic localization of the EZH2 protein induced by As^{3+} in BEAS-2B cells transfected with GFP-EZH2. H$_2$O$_2$ was used as a control of ROS. (C) Statistical analysis of the cytoplasmic translocation ratio of the EZH2 protein in the cells treated with As^{3+} in the presence or absence of NAC. Data are expressed as the mean ± SD, n = 3, ** p < 0.05.

H$_2$O$_2$ could transiently induce the increase of both phosphorylated and total EZH2 in the cytoplasm (Fig. 2.2.4 B). However, this effect of H$_2$O$_2$ was rapidly diminished after 10 min of H$_2$O$_2$ treatment, possibly due to the fast elimination of

H$_2$O$_2$ by the medium, the cellular peroxisomes that contain catalase and the cytoplasmic glutathione peroxidase (GPx) and NADPH (Makino et al., 2004).
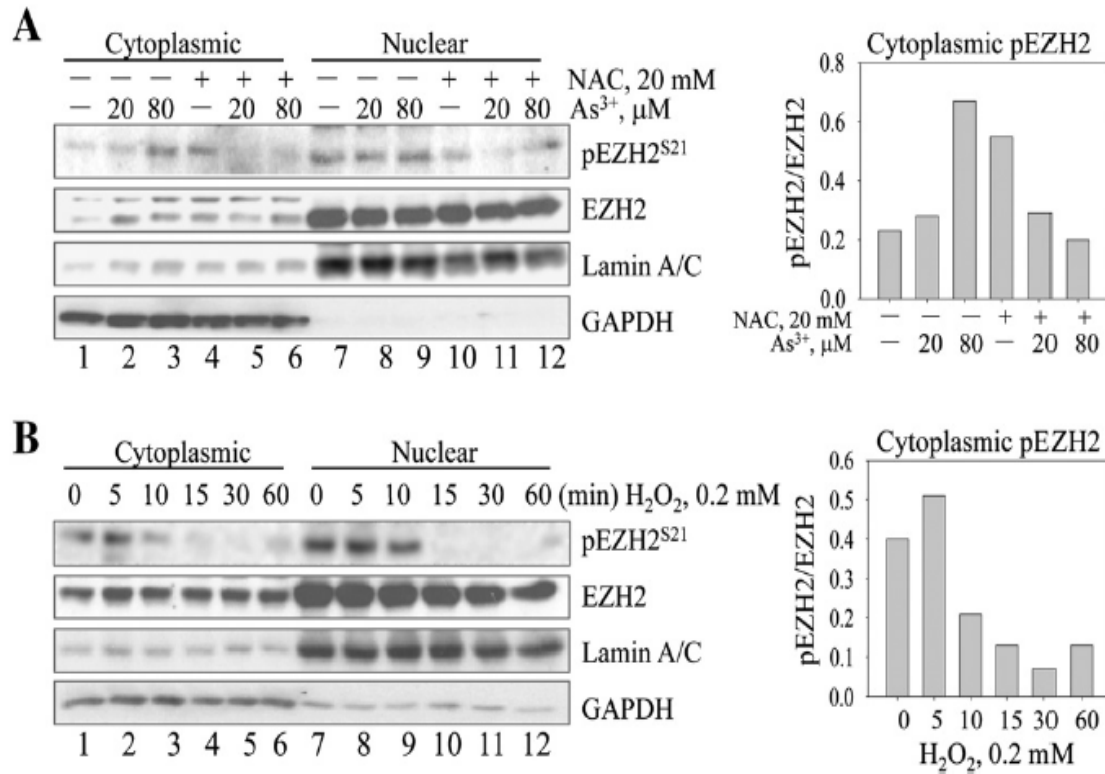
Figure 2.2.4 Increased cytoplasmic localization of the phosphorylated and total EZH2 in BEAS-2B cells treated with As^{3+} or H$_2$O$_2$.

(A) BEAS-2B cells were treated with 20 or 80 µM As^{3+} for 2 h with or without NAC pretreatment. Cellular fractions were made to extract the cytoplasmic and nuclear proteins. Lamin A/C and GAPDH were used as indications of the nuclear and cytoplasmic fractions. Lanes 4 and 10 are NAC only groups. Right panel shows semi-quantification of the ratio between pEZH2 and EZH2 in the cytoplasm. (B) BEAS-2B cells were treated with 0.2 mM H$_2$O$_2$ for the indicated

times. The levels of phosphorylated EZH2, total EZH2, lamin A/C, and GAPDH were determined in the cytoplasmic and nuclear fractions, respectively. Right panel shows semi-quantification of the ratio between pEZH2 and EZH2 in the cytoplasm.

So far, our hypothesis on the arsenic-induced EZH2 phosphorylation and cytoplasmic translocation is through ROS accumulation has been confirmed, whereas the direct connection of such biological event with cell malignant transformation has not yet been established, thus for the next steps we investigated the oncogenic relevance of arsenic-induced EZH2 phosphorylation and further compartmental re-localization. To construct the association of such biological event with oncogenic properties or transformed features, we first focused on the probable contributions of cytoplasmic pEZH2 on malignant transformation. We had reported that chronic exposure of sub-lethal arsenic to BEAS-2B cells will lead to the malignant transformation, and those transformed BEAS-2B cells acquired some features of the cancer stem cells, such as increased expression of Oct4, Sox2, Klf4, and Myc (Chang, Chen et al. 2014). Prompted by such findings, it'll be important to investigate the association of pEZH2 and the expression of the stemness markers.

Cancer Stem Cells (CSCs) refer to a small population of tumor cells that have the ability of both self-renewal and differentiation (Bjerkvig, Tysnes et al. 2005). Reports indicate that CSCs are the key for tumor initiation, progression, therapeutic resistance, and metastasis (Jiang, Li et al. 2014). Thus, we

hypothesize that arsenic-induced pEZH2 through oxidative stress may contribute to the acquisition of CSC traits. A growing body of evidence supports that c-myc, one of the key genes for the self-renewal of the CSCs. It has been shown that the 5'-UTR of c-myc mRNA contains an Internal Ribosome Entry Site (IRES) sequence that confers its expression independent to the canonical cap-dependent protein translation process (Stoneley, Paulin et al. 1998, Chappell, LeQuesne et al. 2000, Shi, Sharma et al. 2005). Since we observed cytoplasmic localization of the pEZH2, and there are reports suggesting c-myc upregulation by EZH2, one of the biological function of pEZH2, thus, may promote c-myc and other protein translation through the cap-independent, but IRES-dependent translation.

The IRES refers to a specific nucleotide sequence in the 5'-UTR region of mRNA enabling the cap-independent translation. The IRES-mediated cap-independent translation is a common biological event in virus, albeit the mechanisms in cells are still under investigation(Komar and Hatzoglou 2011), and our present study provides preliminary data suggesting the role of pEZH2 in up-regulating c-myc expression through the IRES, the non-canonical translation mechanism for the first time. In general, the IRES-dependent translation translates proteins when the cells are in growth-arresting and/or apoptotic states. Under these growth disadvantage conditions, the factors important for cap-dependent translation, such as eIF4B, eIF3, eIF2a, and eIF4Gs, are either been degraded or functionally inhibited. When a given mRNA is subjected to IRES-

dependent translation, the canonical initiation factors are dispensable. It is believed that a direct interaction between the IRES and the 40S ribosome occurs along with the so-called IRES trans-acting factors. Well documented evidence suggests that about 10% mRNAs can manage to escape the translational depression circumstances and maintain translation through the cap-independent, namely the IRES pathway (Kozak 2005). To test our hypothesis on the association of cytoplasmic pEZH2 and c-myc expression, we examined the expression of c-myc for both mRNA and protein levels in the cells Akt I and Akt II, two kinases responsible for EZH2 phosphorylation, was silenced by siRNAs. As depicted in Fig. 2.2.5, Akt silencing is accompanied with a significant decrease of the basal and arsenic-induced c-myc proteins without changes of the c-myc mRNA, indicating that translational, rather than transcriptional regulation of the

Akt   signaling   on   c-myc   expression.
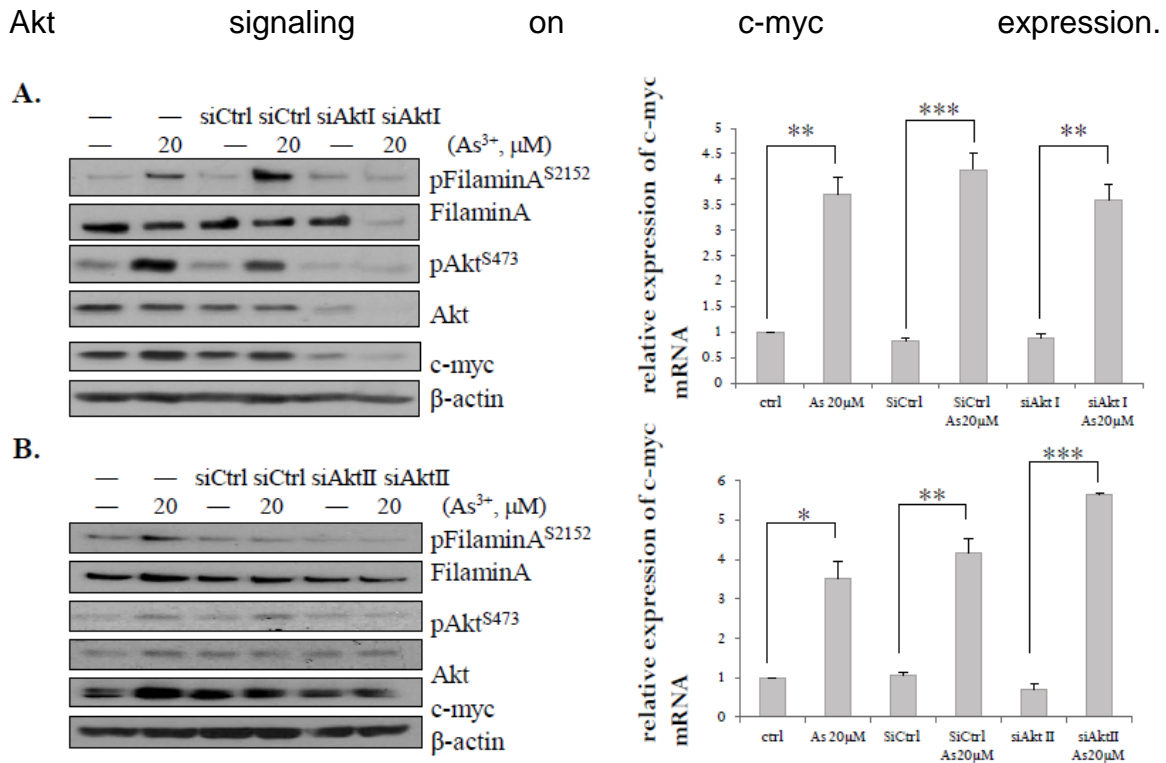
Figure 2.2.5 Involvement of Akt in arsenic-induced c-myc expression.

(A), BEAS-2B cells were transfected with 50nM Control or Akt I siRNAs 24hours before treatment with 20μM arsenic for 2 hours. The expression of the indicated proteins with determined by Westernblotting. Right panel show c-myc mRNA levels determined by qRT-PCR. (B), BEAS-2B cells were under the similar treated as described in (A) with the silencing of Akt II mRNA.

To determine whether Akt regulation on c-myc is through EZH2 phosphorylation and IRES mechanism, we overexpressed a mutated EZH2 in which the serine 21 (S21) was substituted by alanine (S21A) in the BEAS-2B cells. Meanwhile, we also overexpressed another mutated EZH2 in which the S21 was replaced by aspartic acid EZH2 (S21D) that mimics the structure of

pEZH2 on S21. Indeed, the EZH2 S21A was mostly localized in the nuclei of the cells, and EZH2 S21D can be found in both cytoplasm and nuclei (Fig. 2.2.6). Meanwhile, the Western blot analysis also indicates an increased cytoplasmic myc-EZH2 level in the S21D transfected group. These data confirmed our previous findings suggesting that the pEZH2 is more likely to be translocated in to the cytoplasm.
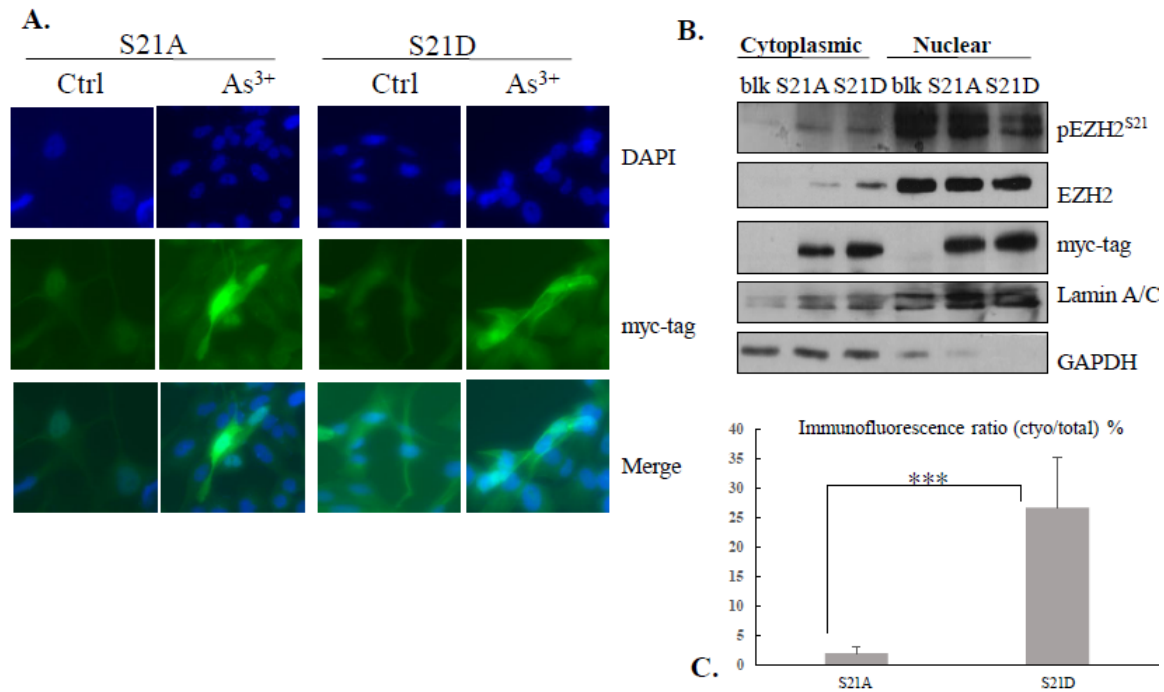
Figure 2.2.6 Cytoplasmic localization of pEZH2.

(A), BEAS-2B cells were transfected with either myc-EZH2 S21A or S21D mutant constructs, with or without 20μM As^{3+} exposure for 2 hours. The transfected cells are further immunostained with myc-tag antibody for microscopic observation and analysis (C). (B), the cytoplasmic and nuclear proteins of the BEAS-2B cells transfected with EZH2 S21A or S21D mutant were isolated separately followed by Westernblotting.

As depicted in Figure 2.2.7A, despite S21 was mutated to A, arsenic was still able to induce EZH2 phosphorylation, indicating that phosphorylation at other sites may occur. Nevertheless, more induction of c-myc protein as well as it down-stream targeting protein mdig. Again, there appeared to be no difference on the c-myc mRNA levels between the cells expressing EZH2 S21A and EZH2

S21D. We also transfected the transformed BEAS-2B cells with EZH2 S21A and EZH2 S21D, respectively. However, a similar level of c-myc protein was noted between the cells expressing EZH2 S21A and EZH2 S21D.
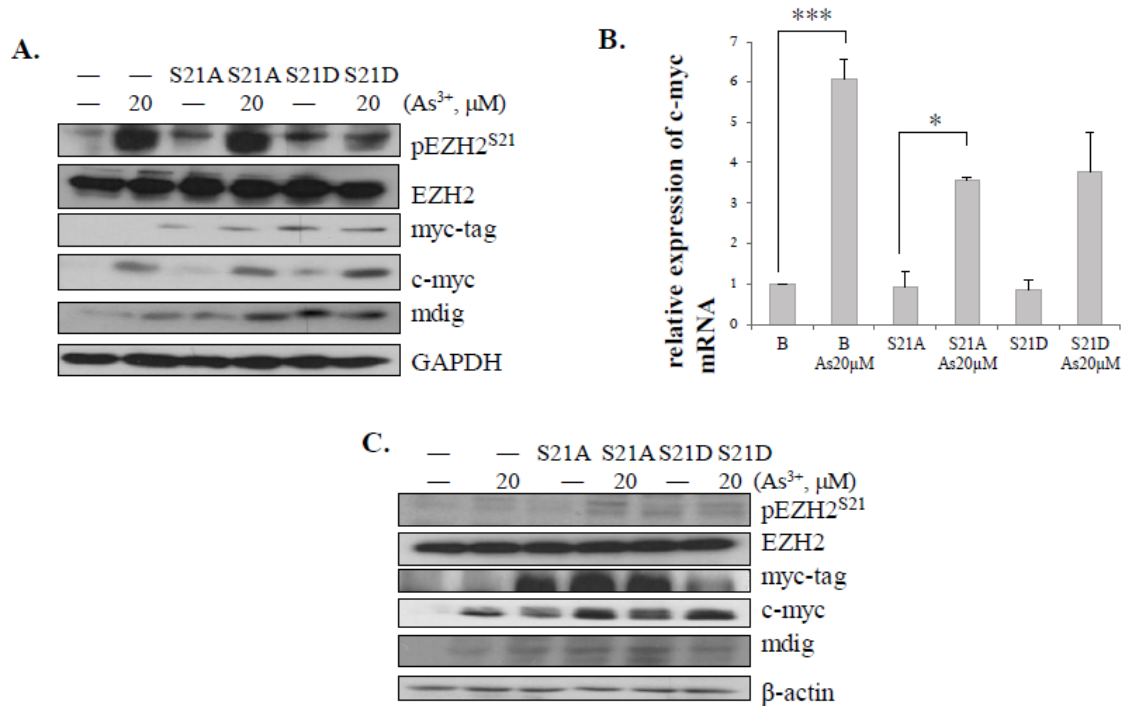
Figure 2.2.7 pEZH2 up-regulates c-myc protein.

(A), BEAS-2B cells were transfected with EZH2 S21A mutant plasmid or EZH2 S21D mutant plasmid 24hours, followed by the treatment with 20μM arsenic for 2 hours. The indicated protein levels were determined by Westernblotting. (B), BEAS-2B cells were under the same treatment as described in (A), and the c-myc mRNA levels were measured by qRT-PCR. (C), Transformed BEAS-2B cells were transfected and treated as the same of the BEAS-2B cells.

The above results are in line with our hypothesis that arsenic-induced EZH2 phosphorylation may up-regulate c-myc protein expression through the IRES-dependent translation. To further address this point, we co-transfected the BEAS-2B cells with an IRES-dependent luciferase reporter vector and EZH2 S21A or EZH2 S21D (Fig. 2.2.8). The IRES-dependent luciferase reporter, pRMF, contains c-myc 5'UTR IRES element at the upstream of firefly luciferase, thus if the c-myc IRES is activated by pEZH2 there will be an increased firefly luciferase luminescence. In the first experiment, we cultured the cells in 5% FBS and then treated with 20μM arsenic. However, we didn't observe an increased c-myc IRES luciferase activity in the cells expressing EZH2 S21D (Figure 2.2.8A). As we had discussed earlier, the IRES-dependent protein translation occurs most likely during the stress condition, such as growth arrest and apoptosis. Thus, we next cultured the cells in 0.5% FBS medium and test the luciferase activities. Indeed, an enhanced luciferase activity was observed in the cells expressing EZH2 S21D relative to the cells expressing EZH2 S21A (Figure 2.2.8A), further suggesting that pEZH2 may promote the IRES-mediated cap-independent translation of the c-myc protein. We speculate that this IRES-based c-myc translation may offset the stress-induced cell death signals. It is true. Cell viability assay using MTT absorption indicated more viable cells of the cells expressing EZH2 S21D than the cells expressing EZH2 S21A (Figure 2.2.8B)
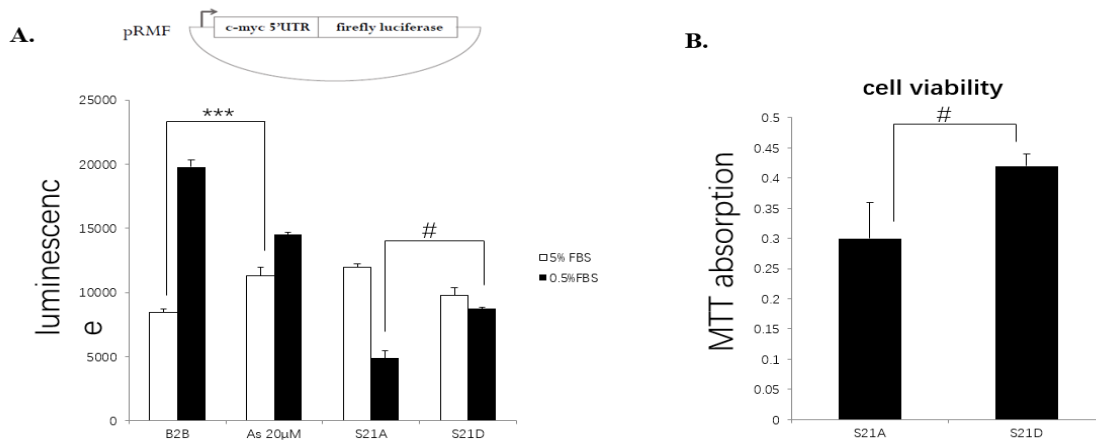
Figure 2.2.8 pEZH2 up-regulates c-myc through IRES.

(A) Plasmid containing the IRES element of c-myc, pRMF, was transfected into BEAS-2B (B2B) cells along with EZH2 S21A or EZH2 S21D EZH2. The luciferase activity was determined for the cells cultured in 5% FBS or 0.5% FBS. (B) pEZH2 improves cell viability. BEAS-2B cells were transfected with either EZH2 S21A or EZH2 S21D and cultured in 0,5% FBS for 24hours. At the end of this culture, cells were subjected to MTT assay to measure the cell viability. ***$p < 0.005$, #$p < 0.001$.

Taken together, above data suggest that the biological consequences of EZH2 phosphorylation are the cytoplasmic translocation of pEZH2. In the cytoplasm, pEZH2 participates in the IRES-mediated, cap-independent protein translation, such as c-myc. Although other mechanisms can not be ruled out, the arsenic-induced c-myc expression may be achieved partially through EZH2 phosphorylation and cytoplasmic localization of the pEZH2, which further enhances IRES-dependent c-myc protein translation. Since c-myc is one of the

pivotal factors for the malignant transformation and generation of the CSCs, the findings of arsenic-induced EZH2 phosphorylation may be more carcinogenic than its non-phosphorylated counterpart.

2.3 Involvement of mi-R214/199a cluster in arsenic-induced cell malignant transformation.

Similar to siRNA, miRNA is a family of small non-coding RNAs that will bind to 3'-UTR region of specific mRNA through base-pairing, leading to translational repression. This group of non-coding RNAs are also able to bind to the open-reading-frame (ORF) or 5'-UTR of mRNAs to induce mRNA degradation, depending on the degree of complementarity. Per the functions of proteins translated from mRNAs that are targeted by miRNAs, miRNAs can be further categorized to tumor suppressor miRNAs and oncomirs. Tumor suppressor miRNAs refer to miRNAs that target mRNAs of oncogenes or growth factors, whereas oncomirs are those miRNAs that can target tumor suppressors. To investigate which groups of miRNAs can be regulated by arsenic, we profiled miRNA expression through both DNA microarray and miRNA microarray for the control BEAS-2B cells and the transformed BEAS-2B cells induced by a six-month arsenic treatment. Table 2.3.1 listed miRNAs that have more than five-fold over-expression in the transformed BEAS-2B cells compared with the control BEAS-2B cells. Among these up-regulated miRNAs, the highest expressed miRNAs are from the miR-214/199a cluster, suggesting the possible oncogenic

roles of these miRNAs in arsenic-induced malignant transformation and carcinogenesis.

miRNAs Name	Fold-Change(Transformed BEAS-2B vs. BEAS-2B
hsa-miR-214-3p	345.978
hsa-miR-199a-3p	121.017
hsa-miR-199a-5p	40.759
hsa-miR-145-5p	13.9976
hsa-miR-10b-5p	11.4962
hsa-miR-196b-5p	11.2852
hsa-miR-34b-3p	9.39436
hsa-miR-10b-5p	9.06381
hsa-miR-146b-5p	8.39626

Table 2.3.1 Fold changes of miRNAs in Transformed BEAS-2B and BEAS-2B cells

MiR-214/199a cluster is located in the opposite strand of intron 14 of dynamin 3 genes, DNM3os, and can be co-transcribed with the host gene or transcribed as an independent transcript (Watanabe, Sato et al. 2008). Limited information is available on the role of miR214/199a in human diseases or cancer. Few earlier studies that miR-214 and miR-199a potentiate the oncogenic roles of Twist (Yin, Chen et al. 2010) and TGF-β1 (Kuninty, Bojmar et al. 2016). The highest expression of miR-214 and miR-199a in the arsenic-transformed cells suggest to us that these two microRNAs may be important in mediating arsenic-induced malignant transformation of the cells.

To validate the microarray data, we first quantified expression of tested miR-214/199a in BEAS-2B and the transformed BEAS-2B through quantitative real-time PCR (qRT-PCR). As indicated in Figure 2.3.1, both miR-214 and miR-199a exhibited more than 6,000-fold overexpression in the transformed BEAS-2B cells relative to the control BEAS-2B cells. In a separate experiment, we also quantified miR-199a-5p and -3p, respectively. Again, a more-than 5,000-fold overexpression of both -5p and -3p was noted in the transformed BEAS-2B cells. Although both -5p and -3p are from the same pri-miR-199a but derived from the opposite strands, the level of -5p is much higher, about 25,000-fold higher in the transformed BEAS-2B cells than the control BEAS-2B cells, possibly suggested differences between miR-199a-5p and miR-199a-3p in their stability and targeting efficiency. Interestingly, both miR-214 and miR-199a were not induced by a short-term arsenic treatment. We treated the control BEAS-2B cells with 20

μM arsenic for 2 hours. However, no induction of miR-214, nor miR-199a, was observed, suggesting a more complicated mechanism is involved in the regulation of the miR-214/199a cluster by arsenic.
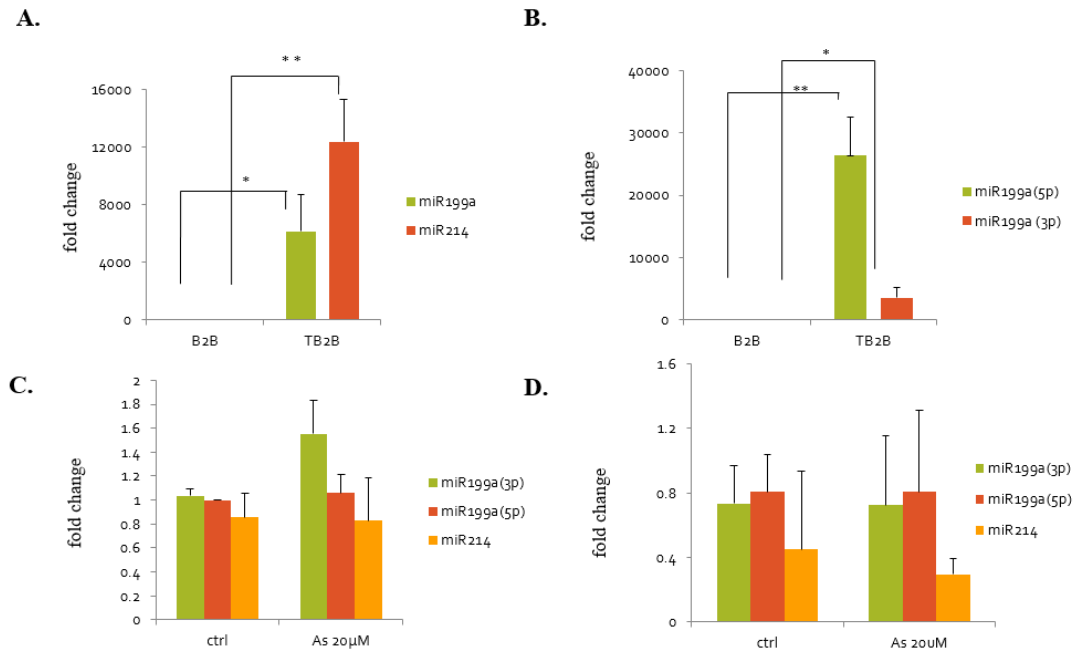
Figure 2.3.1 Involvement of miR214/199a cluster in arsenic-induced malignant transformation.

(A), the expression of mi-R214 and miR-199a were determined in both BEAS-2B (B2B) and Transformed BEAS-2B cells (TB2B) through qRT-PCR. (B), in BEAS-2B and Transformed BEAS-2B cells, the expression of miR199a-5p -3p were tested as described in (A). (C & D), The expression of miR199a-3p, -5p and miR-214 were measured in BEAS-2B cells (C) and Transformed BEAS-2B cells (D) treated with 20μM arsenic for 2 hours. * $p<0.05$, **$p<0.01$.

The inability of short-term arsenic treatment to induce miR-214 and miR-199a expression might be due to the factors of arsenic concentrations. To clarify this consideration, we performed a dose-response study through treating the cells with different concentrations of arsenic for 2 or 72 hours. Again, we did not

observe a significant induction of miR-214 and miR-199a in these additional short-term experiments (Figure 2.3.2)
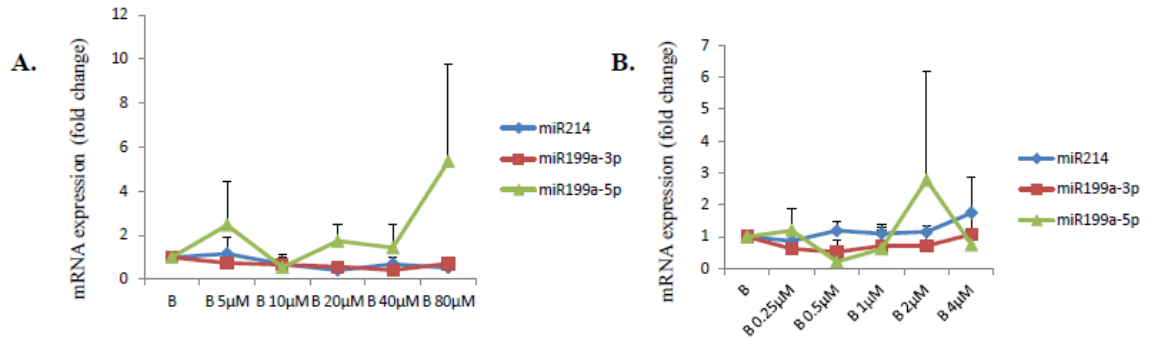
Figure 2.3.2 Influences of short-term arsenic exposure on miR-214 and miR-199a.

(A), BEAS-2B cells were treated with 5 to 80 μM arsenic for 2 hours; (B), BEAS-2B cells treated with 0.25 to 4 μM arsenic for 72 hours. The levels of miR-214 and miR-199a were determined by qRT-PCR.

One of the possibilities that only long-term arsenic treatment is able to induce miR-214 and miR-199a is that transcription of these miRNAs needs some epigenetic changes to cluster located in DNM3os. The most common epigenetic regulation on gene transcription includes DNA methylation and histone modifications, such as acetylation and methylation. Histone acetylation has viewed as a positive marker for transcription (Shukla, Vaissiere et al. 2008), whereas DNA hypermethylation, in general, inhibits transcription (Akhavan-Niaki and Samadani 2013). To that end, we treat BEAS-2B cells with either DNA methyltransferase inhibitor, 5-Aza-2'-Deoxycytidine (5-Aza), or histone

deacetylase inhibitor, Trichostatin A (TSA) for 72 hours, followed by the measurement of miR-214 and miR-199a through qRT-PCR. As shown in Figure 2.3.3, the inhibition of DNA methylation by 5-Aza can promote the expression of miR-214 and miR-199a-3p, and also enable the induction by arsenic, whereas enhancement of histone acetylation by TSA-based inhibition of the HDACs only showed marginal effect on miR-199a and miR-214.
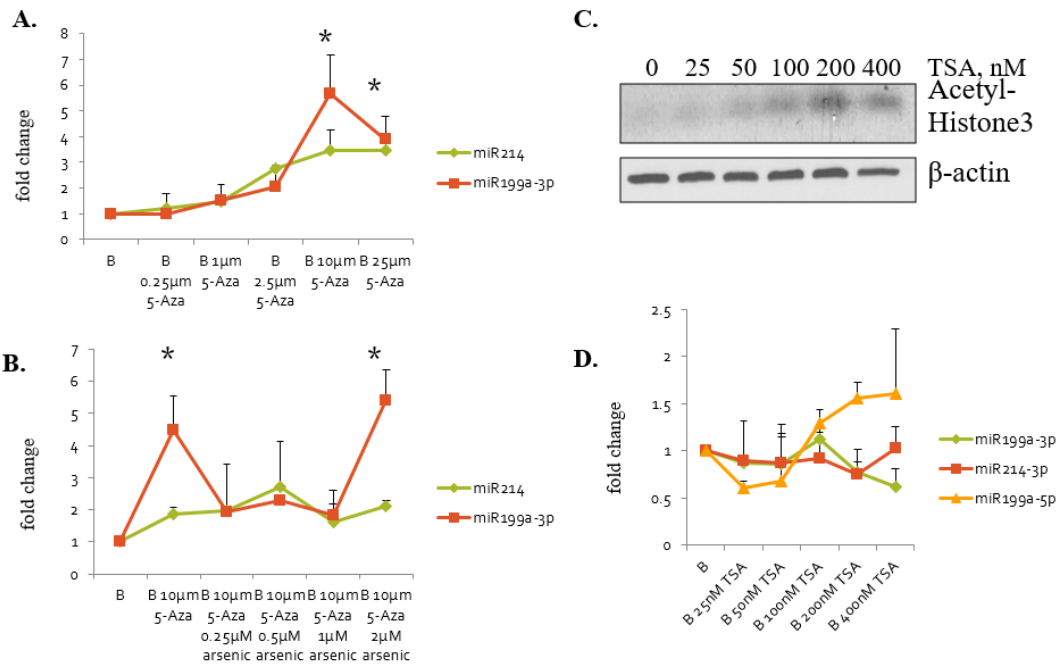
Figure 2.3.3 Role of DNA methylation and histone acetylation in miR-214/199a expression.

(A), BEAS-2B cells were treated with 5-Aza-2'-Deoxycytidine (5-Aza) of the indicated concentrations for 72hours, and the expression of miR-214 and miR-199a-3p were quantified by qRT-PCR. (B), BEAS-2B cells were co-treated with 10µM 5-Aza-2'-Deoxycytidine and the indicated concentrations of arsenic for 72hours, followed by qRT-PCR for miR-214 and miR-199a. (C), BEAS-2B cells were treated with Trichostatin A (TSA) with the indicated concentrations for 72 hours and then measured for histone H3 acetylation by Westernblotting. (D), miR-214 and miR-199a were determined by qRT-PCR in the cells treated with TSA. *$p < 0.05$.

Above data clearly suggest to us that miR-214 and miR-199a must play key roles in the arsenic-induced malignant transformation through serving as oncomirs. It has been known many oncomirs facilitate or promote oncogenesis by down-regulating tumor suppressors, DNA repair proteins, pro-apoptotic proteins. To investigate how miR-214 and miR-199a contribute to the arsenic-induced cell transformation, we developed a comprehensive strategy that contains 3 different steps. At the first step, we performed a bioinformatics mining using 4 different databases to predict the targets of miR-214 and miR-199a, including PITA, MicroRNA.org, Targetscan, and Diana-microt. Since our previous studies already revealed a reduced capacity of ROS induction in the arsenic-induced transformed cells (Chang, Pan et al. 2010), we paid special attention to those targets that are involved in ROS generation, mitochondrial function and energy metabolism. We found all 4 databases predicted both miR-214 and miR-199a can bind to the 3'-UTR of mitochondrial transcription factor A (TFAM). The PITA program even predicted multiple miR-214 and miR-199a binding sites in the 3'-UTR of TFAM, which promoted us to the second step to evaluate whether there are direct physical interactions of TFAM 3'-UTR and miR-214/199a. For that purpose, we transfected the cells with a luciferase reporter construct containing the whole 3'-UTR of TFAM along with precursors or antagomirs for miR-214 and miR-199a. As indicated in Fig 2.3.4, the luciferase activity is decreased in the cells transfected with miR-214/199a precursors as compared with the cells transfected with antagomirs (inhibitors of miR-214 or miR-199a).

These results confirmed the hypothesis that there are direct interactions of both miR-214 and miR-199a with the TFAM 3'-UTR.
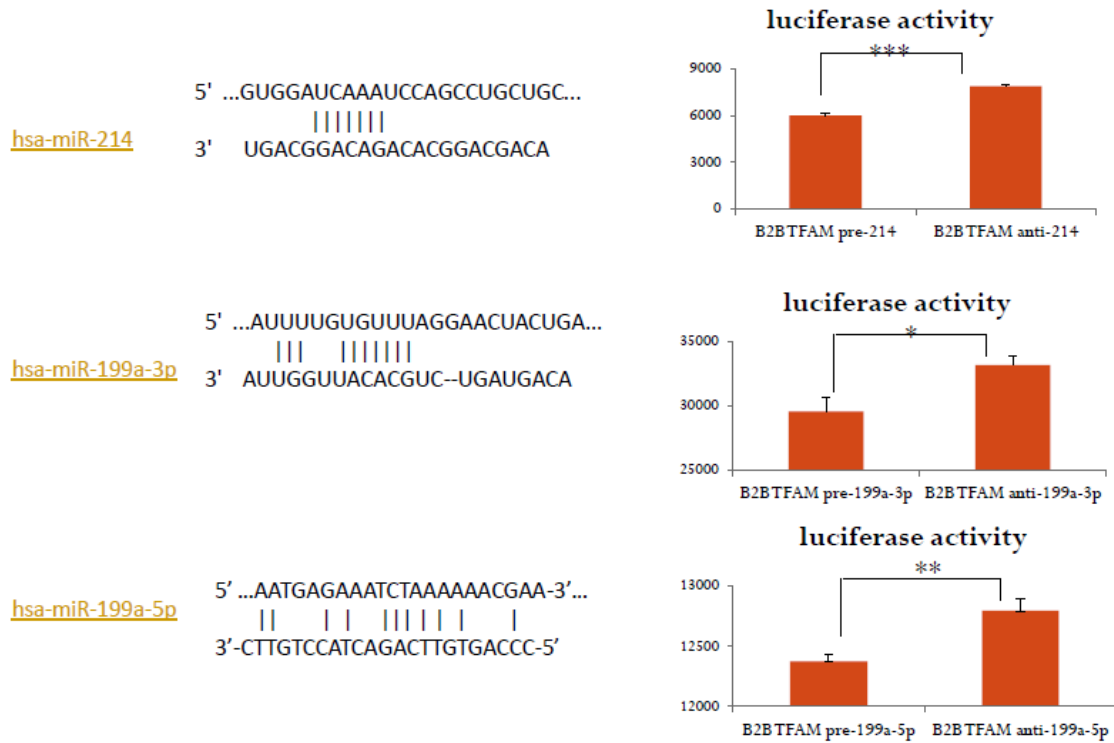
Figure 2.3.4 TFAM is a direct target miR-214 and miR-199a.

BEAS-2B cells were transfected with either miRNA inhibitor or precursor for 24hours, followed by an additional 24hours' culture. At the end of cell culture, total cell lysates were used for luciferase activity assay. *p<0.05, **p<0.01, ***p<0.005.

At the third step, we measured the protein levels of TFAM along with few other mitochondrial proteins, including ND-1, a protein in the mitochondrial respiratory chain and encoded by the mtDNA (mitochondrial DNA), as well as ATP5a and VDAC, which are the typical mitochondrial housekeeping proteins

(Fig 2.3.5). The reason why we focused on the mtDNA-encoded proteins is based on the functional consideration of TFAM. It has been well-established that TFAM can sustain mtDNA replication and transcription by binding to the different regions on mtDNA(Ramos, Santos et al. 2009), thus if miR-214/199a targets TFAM, then the expression of mtDNA-encoded protein should be affected also. The TFAM was readily detected in the control cells. However, we failed to detect the TFAM protein in the arsenic-induced transformed cells were exhibited overwhelming miR-214 and miR-199a expression (Figure 2.3.5). The transformed cells also showed a notable decrease of the expression of ND-1 protein, whereas ATP5a expression was comparable between the control BEAS-2B cells and the transformed cells. Interestingly, VDAC, the mitochondrial membrane protein, was expressed much higher in the transformed cells.
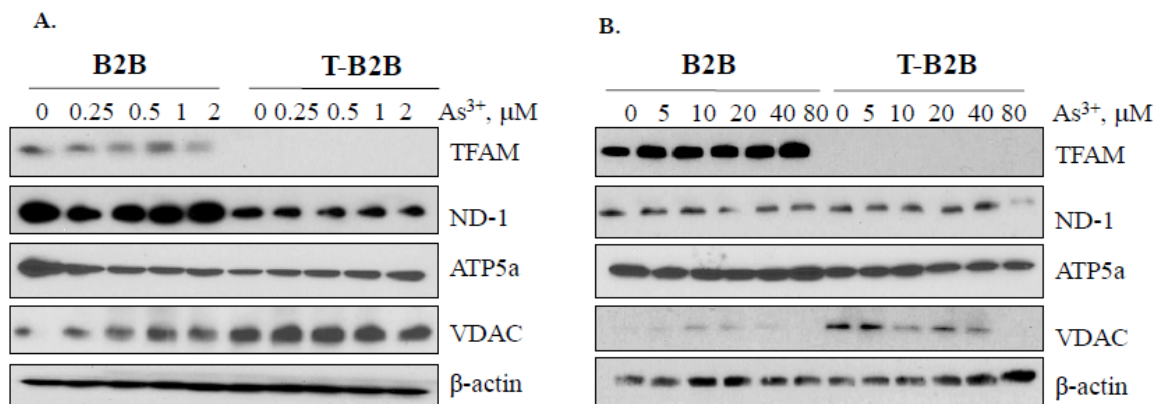
Figure 2.3.5 Decrease of mitochondrial proteins in the arsenic-induced transformed-B2B cells.

(A) The BEAS-2B (B2B) and Transformed BEAS-2B (T-B2B) cells were treated with low dose arsenic as indicated for 72 hours and tested for the protein levels

through Westernblotting using the specific antibodies. (B) Higher concentrations of arsenic were used for a two-hour treatment of the B2B and T-B2B cells. The protein expression determined as described in (A).

Furthermore, we also determined the copy numbers and transcription of mtDNA by PCR in both control cells and the arsenic-induced transformed cells. We used 4 sets of PCR primers to amplify different regions of mtDNA as reported by Ramos et al (Ramos, Santos et al. 2009). As depicted in Figure 2.3.6, a substantial decrease of mtDNA copy number and transcription was observed in the transformed cells, which is in line with the observed decrease of TFAM and increased expression of miR-214 and miR-199a in the transformed cells. Although transfection of the cells with miR-214/199a inhibitors did not recover mtDNA in the transformed cells. The inhibitors did recover TFAM in the control BEAS-2B cells.
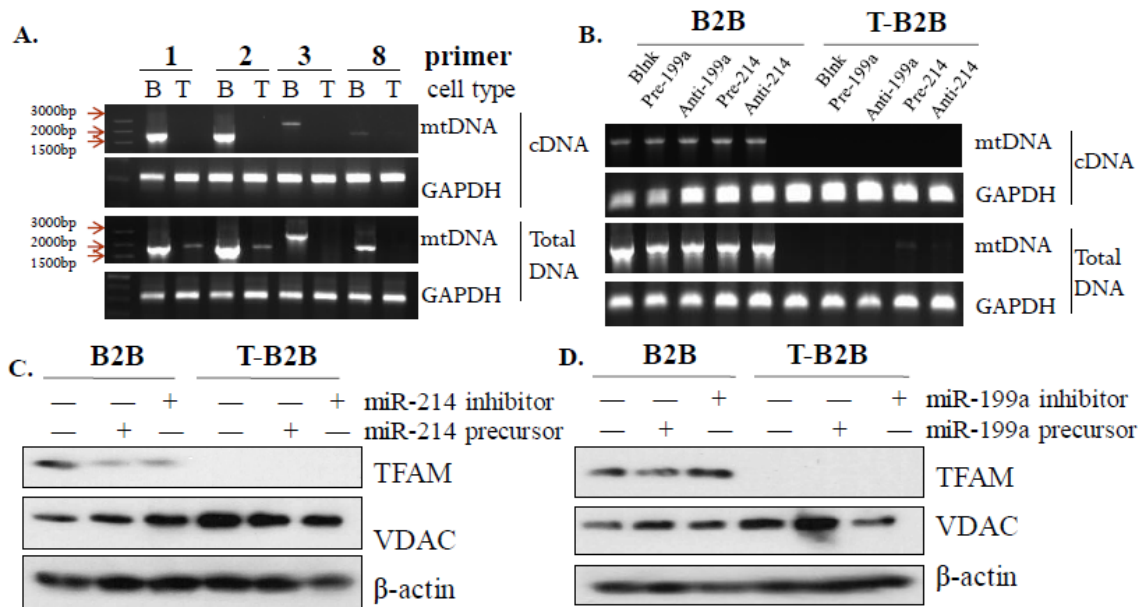
Figure 2.3.6 Regulations of miR214/199a on mtDNA.

(A), Transcription and replication of mtDNA (cDNA) are determined with the primers for different regions on mtDNA (1, 2, 3, 8) in BEAS-2B (B) and Transformed BEAS-2B (T) cells. (B), Recovery test of mtDNA transcription and replication was measured in the control BEAS-2B (B2B) and Transformed BEAS-2B (T-B2B) cells transfected with miR-214 or 199a precursor (pre) or inhibitor (anti). Further protein level of TFAM in B2B and T-B2B cells were tested with the additional miR-214 (C), and miR-199a (D) precursor or inhibitor transfection.

Above data have revealed overexpression of miR-214/199a in the arsenic-induced transformed BEAS-2B cells. These data also provided evidence showing that during the arsenic-induced BEAS-2B cells transformation, the increased miR-214/199a can target TFAM to down-regulate the protein level of TFAM in the transformed cells. Since mitochondrial is the central organelle for glucose and

lipid metabolism, decrease of TFAM by miR-214 and miR-199a will impair the replication, transcription and stability of the mtDNA, leading to malfunction of the mitochondrial metabolism. Thus, it is important to determine is there a metabolic reprogramming in the arsenic-induced transformed cells.

A number of studies revealed unique metabolic features of the cancer cells, stem cells or cancer stem-like cells (CSCs). In general, some of the transformed cells and CSCs exhibit downregulation of mitochondrial respiratory chain complexes, reduction in mtDNA copy number and the immature state of the mitochondria, leading to a reduced oxidative phosphorylation (OXPHOS) and citric acid cycle/tricarboxylic acid (TCA) cycle and an increase in glycolysis (Xu, Duan et al. 2013, Ciavardelli, Rossi et al. 2014). How mitochondrial function and OXPHOS were impaired or inhibited in transformed cells or CSCs is still a mystery. Meanwhile, majority of these studies view this metabolic shift as a byproduct of the cell fate status. In fact, some recent studies had shown that several metabolites from either glycolysis or mitochondrial OXPHOS may be active regulators for the epigenetic modifications and transcriptional regulation involved in self-renewal and lineage commitment of the transformed cells or CSCs, e.g., NAD+ and S-adenosyl methionine (SAM) from glycolysis, acetyl-CoA, α-ketoglutarate (α-KG) and flavin adenine dinucleotide (FAD) from OXPHOS/TCA, are important co-factors or regulators for histone acetylation or deacetylation, histone and DNA methylation or demethylation. Furthermore, O-linked N-acetylglucosamine (O-GlcNAc), a product of subsidiary pathway from

glycolysis, may be essential for the O-GlcNAcylation and activation of Oct4 and Sox2, two key factors for the self-renewal of stem cells and CSCs (Jang, Kim et al. 2012).

To directly demonstrate the metabolic shift, we conducted metabolomics study of the cells by using both ^{13}C glucose flux and untargeted global metabolomics (metabolome) through the DiscoveryHD4 platform for the maximum coverage of the detected changes of metabolites between the control cells and As^{3+}-induced transformed cells. In ^{13}C glucose flux assay, we detected increased glycolytic intermediates G6P/F6P (glucose-6-phosphate/fructose-6-phosphate), FBP (Fructose-bisphosphate), PEP (phosphoenolpyruvate), 2PG/3PG (2-phosphoglycerate/3-phosphoglycerate combined), R5P/X5P (Ribulose 5-phosphate/xylulose 5-phosphate), and others in the transformed cells (Figure 2.3.7). Metabolome study revealed a substantial decrease in the energy (TCA/OXPHOS) metabolism in the As^{3+}-induced transformed cells relative to the control cells (Figure 2.3.8A). As compared with the control or the cells treated with 0.25 μM As^{3+} for 3 days, the most significantly decreased TCA/OXPHOS metabolites in the transformed cells include succinylcarnitine (C4-DC), aconitate (ACO), α-ketoglutarate (α-KG), citrate (CIT), and fumurate (FUM). (Figure 2.3.8B). However, in a short-term treatment of the BEAS-2B cells with 0.25 μM As^{3+} for 3 to 7 days, we observed a time-dependent decrease of FUM and MAL, and a time-dependent increase of CIT and α-KG (Figure 2.3.8C).
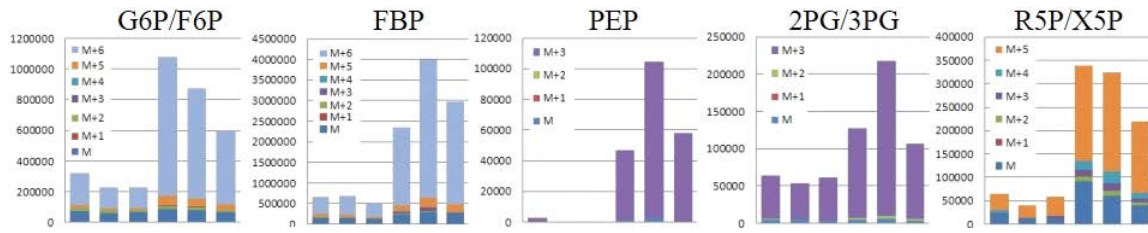
Figure 2.3.7. Changed metabolites in BEAS-2B cells and transformed cells as detected by ^{13}C-Glucose Flux (triplicates of each group).

B: BEAS-2B; T: Transformed cells.
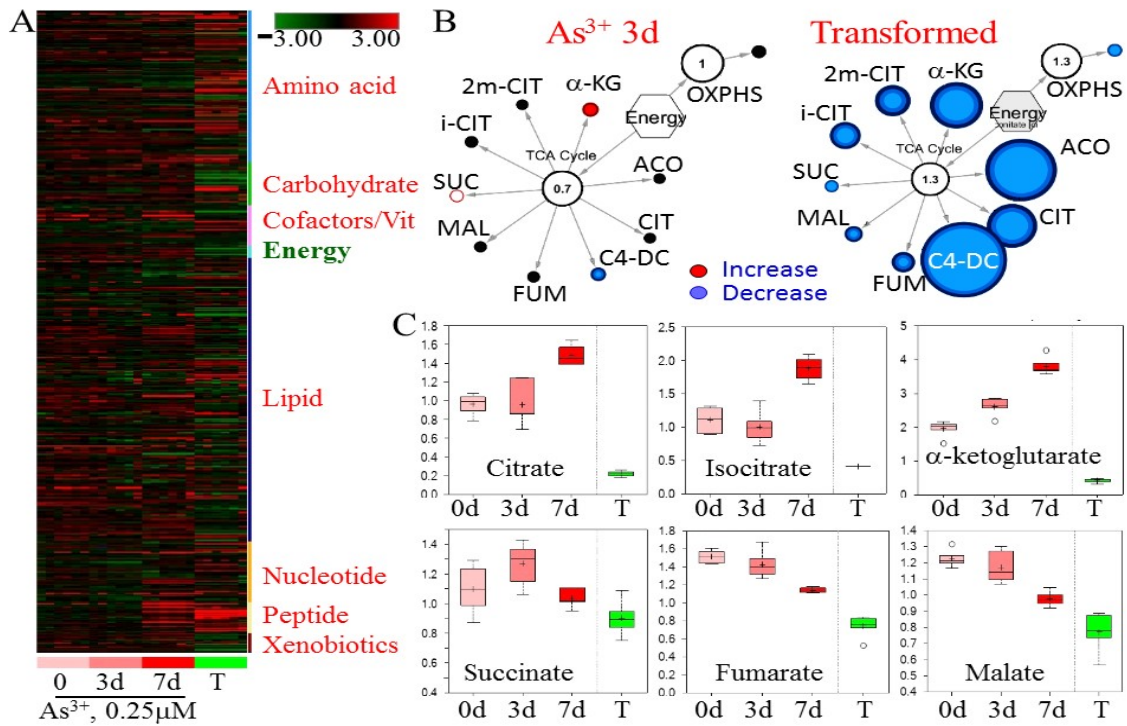
Figure 2.3.8. Altered global metabolomics in transformed cells.

(A) Heat map of metabolites of the control cells treated with 0.25 μM As^{3+} for 0, 3, or 7 days and the As^{3+}-induced transformed cells, n=6; (B) Decreased metabolites in TCA cycle in transformed cells. The sizes of blue circles indicate degrees of decrease. (C) Actual values of the TCA metabolites among the tested cells as indicated. T: transformed cells.

2.4 Discussion

The aim of this dissertation was to explore how arsenic induces cell malignant transformation, by focusing on the epigenetic regulation, such as histone methyltransferase EZH2 phosphorylation, miRNA expression and metabolic changes of the cells in response to arsenic treatment. Abnormalities in epigenetic regulation have been linked to a number of human diseases, the initiation, progression and other pathogenesis of cancers. The most studied epigenetic mechanisms include DNA methylation, miRNAs, histone methylation, histone acetylation, histone phosphorylation, histone ubiquitination, histone sumoylation, histone biotinylation, etc. (Wang, Xin et al. 2016). In this dissertation, much effort was made on arsenic-induced ROS generation that was linked to EZH2 phosphorylation and the subsequent IRES-dependent translation of the oncogene c-myc.

We provided evidence showing that the oxidative stress due to ROS generation contributes to As^{3+}-induced kinase activation that leads to S21 phosphorylation of the EZH2 protein. Meanwhile, oxidative stress appears to be able to induce cytoplasmic localization of the phosphorylated EZH2 protein in the cells treated with As^{3+}. Pretreatment of the cells with NAC prevented EZH2 phosphorylation and cytoplasmic localization induced by As^{3+}. EZH2 is the enzymatic component that forms polycomb repressive complex 2 (PRC2) with EED, SUZ12, RbAp46/48, and possibly other proteins. PRC2 catalyzes the trimethylation of lysine 27 of histone H3 (H3K27me3), a mark of transcriptionally

silent or poised chromatin (Margueron and Reinberg, 2011). In the past few years, EZH2 had been the focus of a significant number of biochemical and molecular studies in cancer cells and cancer stem cells. Many independent studies revealed that EZH2 is overexpressed in several common cancers and that the degree of EZH2 overexpression is associated with the aggressiveness of these tumors (Hock, 2012). Such an overexpression of EZH2 was viewed as a major causative force, rather than a result, of the cancer development. Some genetic studies suggested that missense mutation in the catalytic domain causes hyperactivation of the EZH2 protein and increased incidents of malignancies, such as neuroblastoma and lymphoma (Crea, 2012). Additional evidence also indicated that the overactivation of EZH2 is responsible for the increased aggressiveness of the breast cancer associated with the loss of BRCA1 tumor suppressor (Wang and Huang, 2013). In human prostate cancer, EZH2 is one of the most important oncogenic factors for the initiation and progression of the tumor, as revealed by the fact that the inactivation of EZH2 by chemical inhibitor DZNep reduced tumor size and invasion significantly (Deb et al., 2013). A well-accepted and simplified explanation for the oncogenic role of EZH2 is that EZH2 inhibits the expression of tumor suppressor genes and DNA repair genes through the PRC2-dependent establishment of the silent chromatin that enriched with H3K27me3. A most recent study, however, suggested a PRC2-independent role of EZH2 in glioblastoma stem cells (GSC) (Kim et al., 2013). Following Akt mediated S21 phosphorylation, EZH2 can directly bind to and induce methylation

of lysine 180 (K180) of the STAT3 protein, leading to a sustained activation of the transcriptional activity of the STAT3 and the maintenance of the stemness of the GSC (Kim et al., 2013). S21 phosphorylation of EZH2 by Akt kinase has been first demonstrated in breast cancer cells treated with insulin-like growth factor I (IGF-I) or estrogen (Bredfeldt et al., 2010; Cha et al., 2005). In BEAS-2B cells, we had also noticed S21 phosphorylation of the EZH2 protein through the activation of the JNK-STAT3-Akt signaling axis in response to As^{3+} (Chen et al., 2013).

Arsenic has been shown to be highly capable of inducing ROS generation in a wide range of cell types. The data presented in this dissertation suggested an involvement of oxidative stress or ROS in the As^{3+}-induced EZH2 phosphorylation, which confirmed our previous findings showing that As^{3+} is able to induce ROS generation in the non-transformed BEAS-2B cells (Chang et al., 2010). Further experimentation suggested that the phosphorylated EZH2 may contribute to the IRES-dependent translation of the c-myc oncogene. C-myc has been widely recognized as a promoter for cell proliferation (Kelly and Siebenlist 1985, Lemaitre, Buckle et al. 1996). Indeed, cell viability test revealed cyto protective role of the cytoplasmic pEZH2 when the cells were cultured in the lower FBS (Fig.2.2.8 B). Thus, these findings established an additional oncogenic pathway induced by arsenic, that is arsenic-induced ROS may serve as an initial signal for the kinase activation and EZH2 phosphorylation, and the

phosphorylated EZH2 may contribute to c-myc oncogene translation through the IRES-dependent mechanism.

Extensive studies had been made in the past few years on the role of non-coding RNAs, especially the miRNAs, in the fine-tune regulation of genes and epigenetics under physiological and pathological conditions. It might be the first discovery that long-term treatment of the bronchial epithelial cells (BEAS-2B) induced overexpression of miR-214 and miR-199a that are able to down-regulate TFAM, leading to functional compromising of the mitochondria and metabolic shift of the cells. Metabolic reprogramming from mitochondrial OXPHOS/TCA to cytoplasmic glycolysis has been viewed as major driving force the carcinogenesis and the generation of the cancer stem-like cells. Thus, these findings expanded our view on the mechanisms of arsenic-induced malignant transformation of the cells, that is, along with ROS and kinase-dependent EZH2 phosphorylation and IRES-dependent c-myc translation, the impacts of miR-214 and miR-199a on TFAM and mitochondrial dysfunction may serve as a parallel pathway in cooperation with the ROS-pEZH2-c-myc pathway for the arsenic-induced carcinogenesis.

2.5 Materials and Methods

2.5.1 Cell lines and reagents -- The human bronchial epithelial cell line BEAS-2B was obtained from the American Type Culture Collection (ATCC, Manassas, VA). The BEAS-2B cells were cultured in Dulbecco's modified Eagle's medium (DMEM, Invitrogen, Grand Island, NY) containing 5% fetal bovine serum (FBS, Invitrogen), 1% penicillin/streptomycin, and 1% L-glutamine (Sigma, St. Louis, MO) at 37 °C humidified incubator with 5% CO_2. The cells were treated with As^{3+} [arsenic (III) chloride, Sigma-Aldrich, St. Louis, MO], with the indicated concentrations and time when the cells reached an approximately 80% confluence. In some experiments, ROS scavenger N-acetyl-cysteine (NAC) were added 2h prior to As^{3+} treatment.

2.5.2 Plasmid preparation and transfection -- Constructs of pcDNA3-3myc-6His-EZH2 21D (S21D) and pcDNA3-3myc-6His-EZH2 21A (21A) were purchased from Addgene (Cambridge, MA). The plasmid DNA was amplified in DH5α Competent cells (Invitrogen, Grand Island, NY) and purified using HQ Mini Plasmid Purification Kit (Invitrogen) according to the manufacturer's protocol. Cells in 6-well plates were transfected either with 50 ng plasmid DNA using Lipofectamine RNAiMAX Transfection Reagent (Invitrogen) or 2µg plasmid DNA with Nucleofector (Lonza, Anaheim, CA) with program G016.

2.5.3 Cellular fractionation and Western Blotting -- For nuclear and cytoplasmic fractionations, a NE-PER nuclear and cytoplasmic fractionation kit (Thermo Scientific, Rockford IL) was used according to the manufacturer's

protocol. Fractions were then analyzed by regular Western blotting using GAPDH and lamin A/C as cytoplasmic and nuclear reference, respectively. For regular Western blotting, the cell lysates were prepared by RIPA cell lysis buffer (Cell Signaling, Danvers, MA) followed by ultrasonication and centrifugation. The supernatants were aspirated and proteins were quantified using a SpectraMax spectrophotometer (MDA Analytical Technologies). LDS sample buffer (Invitrogen) and dithiothreitol were added before denature. The samples were separated on 7.5% SDS-PAGE running gel and then transferred to PVDF membranes. The membranes were blocked in 5% non-fat milk in TBST and incubated with the indicated primary antibodies at 4 ℃ overnight, and then incubated with second antibodies at room temperature for 1 h or 4℃ for 4 hours and washed with TBST 3 times for 10 min each. The protein levels were detected using either SuperSignal West Pico (Thermo Fisher Scientific, Waltham, MA) or Immobilon Western chemiluminescent HRP substrate (MILLIPORE, Billerica, MA). The primary antibodies used in Western blotting include anti-phospho-Akt (Ser473) (Cell Signaling), anti-phospho-Filamin A (Cell Signaling), anti-Filmain A (Cell Signaling), anti-Akt (Cell Signaling), anti-myc tag, (Cell Signaling), anti-GAPDH (Cell Signaling), anti-β-actin (Sigma), anti-phopho-EZH2(Ser21) (Abcam), anti-phospho-JNK (Cell Signaling), anti-phospho-Stat3(Ser 727) (Cell Signaling), anti-phospho-p38 (Cell Signaling), anti-phopho-ERK (Cell Signaling), anti-EZH2 (Cell Signaling), anti- JNK (Cell Signaling), anti-Stat3 (Cell Signaling), anti-p38 (Cell Signaling), anti-ERK (Cell Signaling), anti-

GFP (Santa Cruz), anti-Lamin A/C (Santa Cruz), anti-c-myc (Cell Signaling), anti-mdig (Invitrogen), anti-TFAM (Cell Signaling), anti-MT-ND1(Novus Biologicals), anti-ATP5a (Santa Cruz), anti-VDAC (Cell Signaling), and anti-Twist (Santa Cruz).

2.5.4 siRNA Transfection -- Cells with a concentration of 1×10^5/ml were seeded into 6-well plates and transfected with siRNAs using Lipofectamine RNAiMAX reagent (Invitrogen). For short term treatment, 20 μM As^{3+} was added at 24 h and cultured for an additional 2h. Control siRNA and siRNA specifically silencing Akt I and II were purchased from Cell Signaling (Beverly, MA).

2.5.5 RT-PCR-- Total RNA was prepared by lysing the cells with TRIzol reagent (Invitrogen) according to the manufacturer's protocol. The rapid isolation of mammalian DNA was prepared according to the protocol from Molecular Cloning. The reverse transcription and PCR were performed using Access Quick RT-PCR System (Promega) with 2 µg of total RNA and 0.3 µM sense and anti-sense primer. The mtDNA primer sequences as described in Dr. Ramos' previous study(Ramos, Santos et al. 2009). The GAPDH primer sequences are: sense: 5′-CTGAACGGGAAGCTCACTGGCATGGCCT-3′; antisense: 5′-CATGAGGTCCACCACCCTGTTGCTGTAG-3′.

2.5.6 Real-Time PCR-- Total RNA was extracted by TRIzol method and followed by reverse transcription using High-capacity cDNA Reverse Transcription Kits (Applied Biosystems). Each sample contains 0.2 µl dNTPs (100 mM, with dTTP), 1 µl reverse transcriptase, 1.5 µl 10 × reverse transcription buffer, 0.2 µl RNase

inhibitor (20 U/µl), 1 µg total RNA, 5 × RT miR-214 or 199a primer (3 µl) and comparative volume of Nuclease-free water to the total volume of 15 µl. The miRNAs were quantified by real time PCR using TaqMan Small RNA Assays (Applied Biosystems) and 18S rRNA that was used as an endogenous control. For c-myc gene, the primers for reverse transcription are the 2 µl 10× random primers, and further analyzed by real time PCR using c-myc primer as 5'-TACCCTCTCAACGACAGCAG-3' and 5'-TCTTGACATTCTCCTCGGTG-3' and SDHA as an endogenous control. . For TFAM and DNM3os gene, the primers for reverse transcription are the 2 µl 10× random primers, and further analyzed by real time PCR using TFAM primer as 5'-CATCTGTCTTGGCAAGTTGTCC -3' and 5'-CCACTCCGCCCTATAAGCATC -3', meanwhile DNM3os primer as5'-CAGCCCTTGAGTGTGTCTCA-3' and 5'-TACAACGGCATTGTCCTGAA-3' with 18s rRNA (primer 5'-GGCCCTGTAATTGGAATGAGTC -3' and 5'-CCAAGATCCAACTACGAGCTT -3') as an endogenous control.

2.5.7 Luciferase target validation assay-- The cells were seeded in 24-well plates at a density of 5 × 10^4/well. A TFAM (NM_003201) 3'-UTR clone in pMirTarget vector was purchased from Origene. The cells were transfected with the reporter constructs using Lipofectamine 2000 (Invitrogen) 24 h after plating according to the protocol provided by the manufacturer. Twenty-four hours after transfection, the cells were further transfected with miRNA precursor or inhibitor for anther 24 h, and analyzed by luciferase assay using the Luciferase Reporter Assay System (Promega) and a Glomax 20/20 luminometer (Promega). For the

c-myc IRES luciferase activity, the pRMF plasmid is a kind courtesy from Dr. Willis (University of Leicester, UK), and after transfection of pRMF construct for 24 hours, either S21A or S21D EZH2 plasmid (Addgene) is further transfected for another 24 h, and after that the luciferase assay is conducted as described above.

2.5.8 Metabolomics—For glucose flux, 3-4 million cells /sample in 10cm dish with three replicates were prepared, and get every sample exposed with 4500mg/L U-^{13}C glucose DMEM medium for 1 hour labeling (the concentration of glucose is same with the original culture medium glucose concentration). After labeling, remove medium and wash cells with cold 150mM ammonium acetate and get the buffer removed within 30 seconds. Quenching cells by pouring liquid nitrogen on the plate and allow evaporation until the majority of liquid nitrogen is gone. After the quick quench, wrap all of the plates with aluminum foil and store at -80°C or put them on dry ice for shipment, the data were analyzed by University of Michigan Metabolomics or Metabolon Company(Untargeted Global Metabolomics).

2.5.9 MicroRNA inhibitor and precursor -- The BEAS-2B cells or Transformed BEAS-2B cells were first seeded in a density of 2×10^5/ml into 6-well plates at 37 °C with 5% CO_2 for 24 h, then transfected with 60 nM miRNA precursor or inhibitor (Invitrogen) with Lipofectamine RNAiMAX reagent (Invitrogen). Opti-MEM I Reduced Serum Medium (Invitrogen) was used to dilute nucleic acid and

liposome as suggested by the manufacturer. Protein levels were determined by Western blotting as described above.

2.5.10 MTT cell viability assay – BEAS-2B cells were seeded in a 96 well plate with 10,000 cells each well, and after 24 hours of culture in 0.5% FBS supplemented medium, S21A or S21D EZH2 constructs were transfected to the cells according to the protocol for 24 hours. After 24hours of transfection, 10ul of 5mg/ml MTT (3-(4,5-Dimethylthiazol-2-yl)-2,5-Diphenyltetrazolium Bromide) (MP Biomedicals,LLC) was added into each plate for 3hours' incubation at 37 $^\circ$C incubator, and after incubation, aspirating medium and adding 100ul DMSO (Dimethyl sulfoxide) (Fisher Scientific) each well for further 30min shaking and after that absorbance was read at 570nm (formazan) and 690nm (reference) by Synergy H1 hybrid Reader (BioTek).

2.5.11 Statistics-- Microsoft Excel was used for statistical analyses of the quantitative data. The data are expressed as the mean ± standard deviation (SD), and Student's t-tests were used to determine the statistical significance of differences between samples treated under different conditions. Differences were considered statistically significant when $*p < 0.05$.

CHAPTER 3 CONTRIBUTIONS OF ARSENIC-INDUCED CELL MIGRATION AND INVASION TO THE MALIGNANT TRANSFORMATION

CHAPTERS CONTAIN MATERIAL FROM PUBLISHED WORK IN WHICH I WAS THE FIRST AUTHOR. THE CO-AUTHORS OF THESE PUBLICATIONS AGREE TO THE USE OF THE PUBLISHED DATA IN THIS DISSERTATION.

3.1 Introduction

In this chapter, we will discuss a relatively downstream effect of the arsenic-induced malignant transformation, the metastasis and invasion. Metastasis refers to a process that cancer cells migrate to the secondary site(s) from their original tumor site, which occurred in almost all cancers that progressed to later stages. The first step of metastasis is the cell motility that drives cancer cell migration. Thus, we will aim at the underlying mechanisms of arsenic-induced cell migration and invasion. In human bronchial epithelial cells or lung cancer cells, we had shown that As^{3+} is able to activate protein kinase Akt through either inducing miR-190 or initiating the signaling cascade from JNK to STAT3 that contributes to Akt-dependent EZH2 phosphorylation, cell transformation and/or migration (Beezhold, Liu et al. 2011, Liu, Chen et al. 2012, Chen, Liu et al. 2013). Akt has long been viewed as a master regulator of epithelial-mesenchymal transition (EMT), cancer cell migration, invasion, and metastasis(Jiang and Liu 2009, Xue, Restuccia et al. 2012). Akt can directly phosphorylate ACAP1, Pak1, POSH, Girdin, and Twist that contain R-X-R-X-X-S/T or R-X-X-S/T Akt phosphorylation motif, followed by integrin recycling, actin cytoskeleton remodeling and

EMT(Manning and Cantley 2007, Dillon and Muller 2010). Hence, we hypothesized that pAkt substrate that responds to arsenic may be the regulator for arsenic-induced cell migration and further metastasis. Furthermore, ample evidence also indicates a positive role of ROS in cell motility enhancement (Nguyen, Zucker et al. 2011, Singh, Shankar et al. 2014).

In addition to the capabilities of cancer cells in proliferation and apoptotic responses for colonization at the secondary site, the key event of metastasis is the cytoskeleton remodeling, detachment, polarization, and mobilization of the cells (Wu, Wu et al. 2008). In non-muscle cells, filamin A was the first discovered actin-filament crosslinking protein that interacts with integrins and several other cytoskeleton remodeling proteins (Nakamura, Stossel et al. 2011, Wickstead and Gull 2011, Savoy and Ghosh 2013). Intriguingly, this protein has also been confirmed as a substrate for some protein kinases, including FAK, Lck (Goldmann 2002), PAK1 (Hammer, Rider et al. 2013), MAPK (He, Kole et al. 2003), and Akt (Ravid, Chuderland et al. 2008), indicating that phosphorylation of filamin A is an essential step in initiating filamin A interaction with the cytoskeleton remodeling proteins or integrins for cell migration (Chen, Kolahi et al. 2009). In this chapter, we will further investigate the As^{3+}-induced cell migration through ROS-dependent activation of Akt that phosphorylates filamin A at serine 2152 in human bronchial epithelial cell line, BEAS-2B.

3.2 Identification of Filamin A as the putative substrate for pAkt responsible for arsenic-induced cell migration.

During the processes of our research on the role of p-EZH2 in arsenic mediated signaling pathways, we hypothesized that arsenic induces EZH2 phosphorylation and translocation through Akt activation. As an arginine (Arg, R)-directed or AGC-family kinase, Akt can directly phosphorylate serine (Ser)/Threonine (Thr) in a conserved motif, RXRXXS/T, characterized by R at positons −5 and −3 (Alessiet al., 1996). Accordingly, proteins containing RXRXXS/T motif can be phosphorylated by Akt, which can be recognized by anti-RXRXXS*/T* motif antibody (anti-Akt substrate antibody, "*" indicates phosphorylation). The human EZH2 protein contains RKRVKS21 motif that is in consensus with the conserved Akt phosphorylation site. To determine if As^{3+} can induce S21 phosphorylation of the exogenous EZH2 by Akt, the HEK-293 cells were transfected with a 3myc-tagged EZH2 followed by As^{3+} treatment. In the Western blotting results as shown in Fig. 3.2.1 A, the anti-Akt substrate antibody detected several bands with molecular weights around 170, 130, 95, 72, and 50 kDa (Fig. 3.2.1 A, pointed by small triangles) in the cells treated with As^{3+}.

To test whether these Akt substrates are also present in other types of cells in response to As^{3+}, we performed IP analysis using cell lysates from HEK-293 cells cultured in the absence or presence of 20 µM As^{3+} for 2 h and an antibody specifically recognizing the phosphorylated Akt phosphorylation motif, R-X-R-X-X-S/T. As depicted in Fig. 3.2.2A, a band with an estimated molecular weight about 280 kDa was constitutively detected in HEK-293 cells (pointed with a black block arrow). Treatment of the cells with As^{3+} enhanced the density of this band

considerably. Pre-incubation of the cells with an antioxidant, NAC that scavenges reactive oxygen species (ROS), diminished this band completely, suggesting that the occurrence of this band is ROS-dependent. To determine the nature of this protein band that can be recognized by an anti-Akt phosphorylation substrate antibody, we retrieved this band from Western blotting membrane and subjected it to proteomics analysis through tryptic digestion and peptide identification using orbitrap Fusion mass spectrometry as described under Materials and Methods. The peptides identified from this analysis suggested a possible presence of 11 proteins in this protein band as detected in IP, among which only two proteins, filamin A and inositol 1,4,5-trisphosphate receptor type 3 (ITPR3), are within the range of molecular weight between 200 and 300 kDa where the original band was positioned. The filamin A was represented by 10 peptides, whereas ITPR3 was represented by only 4 peptides. Thus, we concluded that the most abundant protein in this IP band is filamin A based on the assumption that the number of peptides identified in mass spectrometry is generally proportional to its abundance or concentration in the sample.
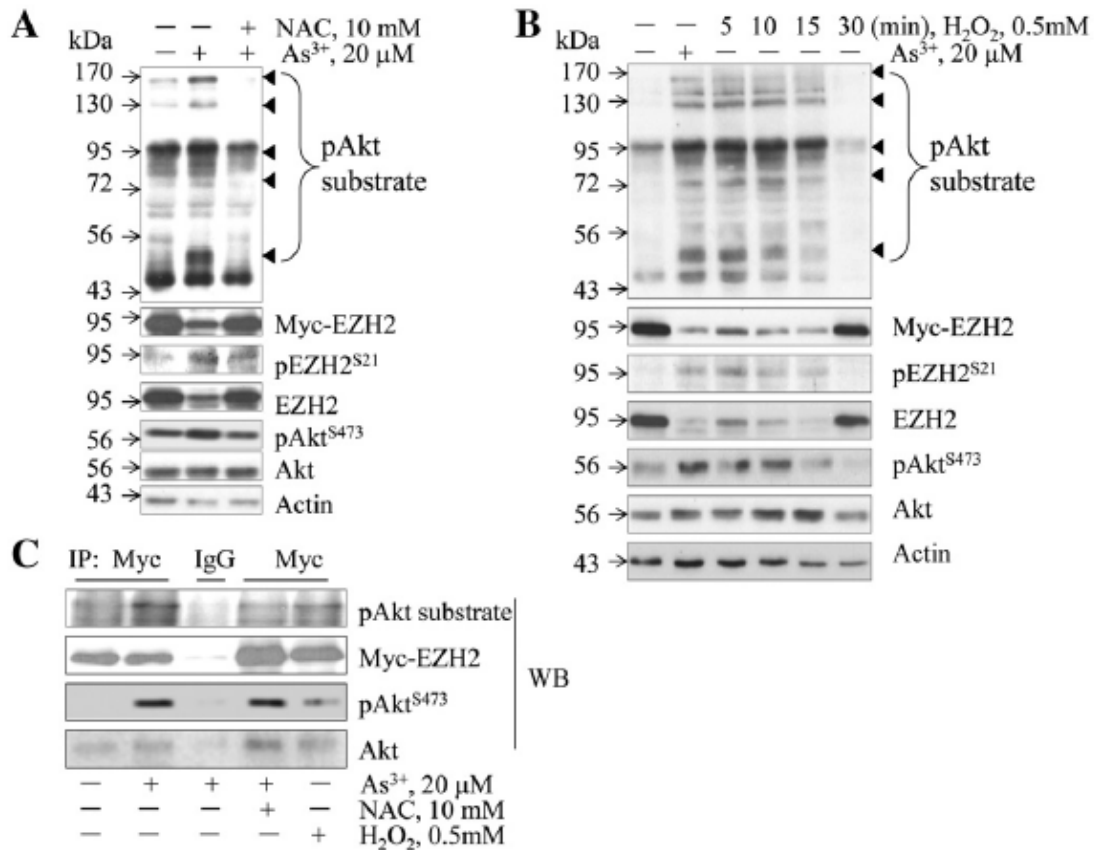
Figure 3.2.1 Both As^{3+} and H$_2$O$_2$ induce the interaction of Akt and EZH2 and Akt-dependent phosphorylation of the exogenous EZH2 overexpressed in HEK-293 cells.

(A) HEK-293 cells were transfected with 3myc-tagged EZH2 expression vector for 24 h followed by the treatment of the cells with 20 μM As^{3+} for 2 h in the presence or absence of 10 mM NAC, followed by Western blotting using the indicated antibodies. (B) The transfected HEK-293 cells were treated with As^{3+} or H$_2$O$_2$, followed by Western blotting as in (A). (C), Anti-myc tag or control IgG was used in immunoprecipitation (IP) to pull down the exogenous myc-tagged EZH2.

The IP was then subjected to Western blotting using antibodies recognizing the phosphorylated Akt substrate motif (RXRXXS*/T*), myc tag, pAkt, and Akt.

To further confirm filamin A as an Akt substrate, we next determined whether there is a direct interaction between protein kinase Akt and filamin A in BEAS-2B cells treated with As^{3+} through immunoprecipitation. Again, the anti-Akt substrate antibody was able to pull down filamin A in the cells treated with As^{3+} (Fig. 3.2.2C, top two panels). Using antibodies against either the total Akt or phospho-Akt (pAkt), we showed that both activated and total Akt were able to interact with filamin A that was phosphorylated at serine 2152 (S2152), and this interaction occurred only in the cells treated with As^{3+} but not the cells without As^{3+} treatment (Fig. 3.2.2 C). To exclude the possibility of non-specific protein-protein interaction during IP, we also used control IgG in our immunoprecipitation assay. It is clear that only the anti-pAkt antibody, but not IgG, can pull down the phosphorylated filamin A (Fig. 3.2.2 D). Therefore, these data provided substantial evidence indicating that filamin A is an endogenous Akt substrate that can be phosphorylated by Akt through direct interaction.

Sequences in Filamin A	Actual Mass	Start	Stop
(K)RAEFTVETR(S)	1,107.57	301	309
(K)VTAQGPGLEPSGNIANK(T)	1,651.86	384	400
(K)TGVAVNKPAEFTVDAK(H)	1,644.86	685	700
(K)AFGPGLQGGSAGSPAR(F)	1,428.71	1072	1087
(R)EATTEFSVDAR(A)	1,224.56	1273	1283
(R)GAGTGGLGLAVEGPSEAK(M)	1,569.81	1382	1399
(R)ANLPQSFQVDTSK(A)	1,433.71	1465	1477
(K)KTHIQDNHDGTYTVAYVPDVTGR(Y)	2,586.26	1593	1615
(K)VAQPTITDNKDGTVTVR(Y)	1,813.95	1815	1831
(R)LVSNHSLHETSSVFVDSLTK(A)	2,199.12	2521	2540

Figure 3.2.2 Identifying filamin A as an Akt substrate.

(A), HEK-293 cells were treated with 20 µM As^{3+} in the presence or absence of 10 mM N-acetyl L Cysteine for 2 h. Cell lysates were prepared using non-denature buffer and subjected to immunoprecipitation (IP) using anti-Akt substrate antibody. Block arrow denotes protein band on the PVDF membrane that was retrieved for mass spectrometry analysis. (B), Mass Spectrometry results show the peptide profiling that overlaps sequence of filamin A. Top two

panels are representative spectrums of the peptides from filamin A. (C), BEAS-2B cell were treated as in (A), and subjected to IP using the indicated antibodies followed by Western blotting (WB). (D), BEAS-2B cells were treated with 20 µM As^{3+} for 2 h, followed by IP using IgG or pAkt antibody as indicated and then WB using phospho-Filamin A (pFilamin A) or pAkt antibody.

To extend above observations, we pretreated the cells with Wortmannin, an inhibitor that is relatively specific for the upstream kinase, PI3K that phosphorylates and activates Akt, in the BEAS-2B cells. A dose-dependent inhibition of the As^{3+}-induced filamin A phosphorylation was observed in the cells pretreated with 10 or 20 µM Wortmannin that diminished Akt activation completely (Fig. 3.2.3A). This inhibitor had no detectable effect on the protein levels of non-phospho-filamin A, total Akt or β-actin (Fig. 3.2.3A). The requirement of activated Akt kinase in As^{3+}-induced filamin A phosphorylation was further validated by silencing Akt using siRNA that specifically down-regulates Akt expression. As indicated in Fig. 3.2.3 B, the control siRNA with scramble sequence (siCtrl) has no inhibitory effect, neither on the level of phospho-filamin A (pFilamin A_{S2152}) nor the total Akt. Silencing Akt using Akt specific siRNA (siAkt) not only reduced the levels of total Akt and the activated pAkt, but also attenuated phosphorylation of filamin A in the cells treated with As^{3+}(Fig. 3.2.3 B). Taken together, these data clearly suggest that the As^{3+}-induced Akt activation, as determined by the phosphorylation on serine 473 (S473), is essential for the phosphorylation of filamin A at S2152.

We had previously demonstrated that As^{3+} induces excessive generation of ROS that contribute to Akt activation and the subsequent transformation of the cells(Chang, Pan et al. 2010). To address the role of ROS in As^{3+}-induced filamin A phosphorylation, we first treated the cells with As^{3+} in the absence or presence of 20 mM NAC, a widely-used ROS scavenger. As expected, NAC prevented As^{3+}- induced Akt activation and filamin A phosphorylation (Fig. 3.2.3 C). The role of ROS in As^{3+}-induced filamin A phosphorylation was additionally confirmed by treatment of the BEAS-2B cells with 200 μM H_2O_2 for 5 to 60 min. Indeed, H_2O_2 is able to induce Akt activation and filamin A phosphorylation in a time dependent manner. The activation of Akt and phosphorylation of filamin A can be detected as early as 5 min after the cells treated with H_2O_2. At 30 min, the filamin A phosphorylation reached plateau (Fig. 3.2.3 D).
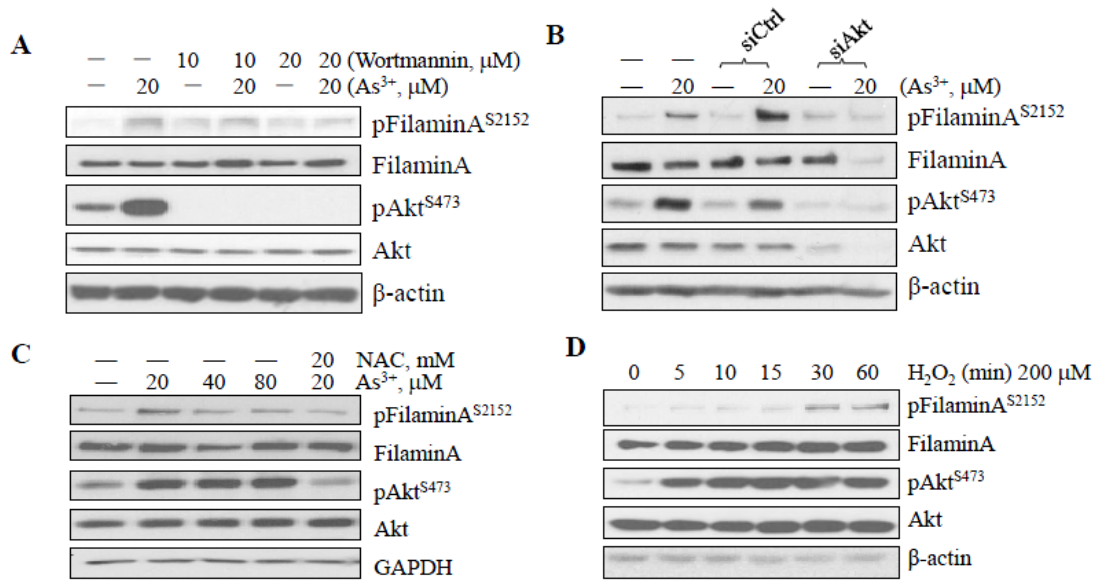
Figure 3.2.3 As^{3+}-induced Akt activation and Filamin A phosphorylation are ROS dependent.

(A), BEAS-2B cells were treated with 20 µM As^{3+} for 2 h with or without pretreatment with 20 µM wortmannin. The protein levels of phospho-filamin AS2152, filamin A, pAktS473, Akt, and β-actin were determined by WB. (B), BEAS-2B cells were transfected with 50 nM Ctrl siRNA or Akt siRNA with or without an additional treatment of As^{3+} for 2 h. WB was then performed as in (A). (C), BEAS-2B cells were treated with the indicated concentrations of As^{3+} and/or NAC. WB was then performed as in (A). (D), Time-dependent induction of Filamin A phosphorylation by H$_2$O$_2$ in BEAS-2B cells.

Accordingly, Filamin A belongs to the Filamin family, which plays a significant role in cytoskeleton remodeling. The three family members are Filamin A, B and C, and among them Filamin A was the first discovered actin-filament

crosslinking protein in non-muscle cells(Savoy and Ghosh 2013), it exerts its function as a cytoskeleton remodeler through several mechanisms, including: (1) crosslinking actin and filaments into systemic network; (2), anchoring the proteins for actin cytoskeleton; (3), interacting with integrins (Chen, Kolahi et al. 2009)and other transmembrane complexes (Rognoni, Stigler et al. 2012). Additionally, Filamin A is also reported to play a critical role in cell motility and migration (Chen, Kolahi et al. 2009, Nakamura, Stossel et al. 2011, Wickstead and Gull 2011). Based on these findings, we propose that arsenic enhances cell locomotion by activating Filamin A.

Activation of Akt has been linked to a number of cellular processes, including cell growth, anti-apoptosis, transformation, migration, invasion, and metastasis of the cancer cells (Cheng, Lindsley et al. 2005). Accordingly, it is plausible to hypothesize that the activation of Akt by As^{3+} can be involved in cell migration. To test this, we first treated BEAS-2B cells with As^{3+} and then measured cell migration capability using Matrigel-based Migration Chambers. As^{3+} treatment promoted cell migration significantly (Figs. 3.2.4 A and C). Silencing Akt using Akt specific siRNA reduced the number of the migrated cells in response to As^{3+}. As^{3+}-induced cell migration was not affected by the control siRNA (siCtrl, Figs. 3.2.4 B and C).

To answer whether filamin A phosphorylation served as a downstream signal for As^{3+}-induced Akt activation that facilitates cell migration, we next silenced filamin A by transfection of the cells with filamin A specific siRNA (siFlna)

followed by measuring the cell migration. Filamin A specific siRNA, siFlna, reduced the levels of both filamin A and the S2152-phosphorylated filamin A (pFilamin AS2152) notably (Fig. 3.2.5 A). The control siRNA, siCtrl, exhibited no significant effects on these proteins, neither pFilamin A, nor total Filamin A. In cell migration assays, again, As^{3+} increased the number of migrated cells significantly (Figs. 3.2.5 B and C). No inhibition of the As^{3+}- induced cell migration was detected in the cells transfected with the control siRNA (siCtrl). In contrast, a strong inhibition of cell migration induced by As^{3+} was observed in the cells transfected with siFlna that specifically silences filamin A (Figs. 3.2.5 B and C). These observations, thus, not only reinforced the notion that filamin A might be an important regulator for cell migration(Ravid, Chuderland et al. 2008, Pena, Arderiu et al. 2012), but also provided strong evidence indicating that filamin A is a downstream effecter to bridge As^{3+}-induced Akt activation and migration.
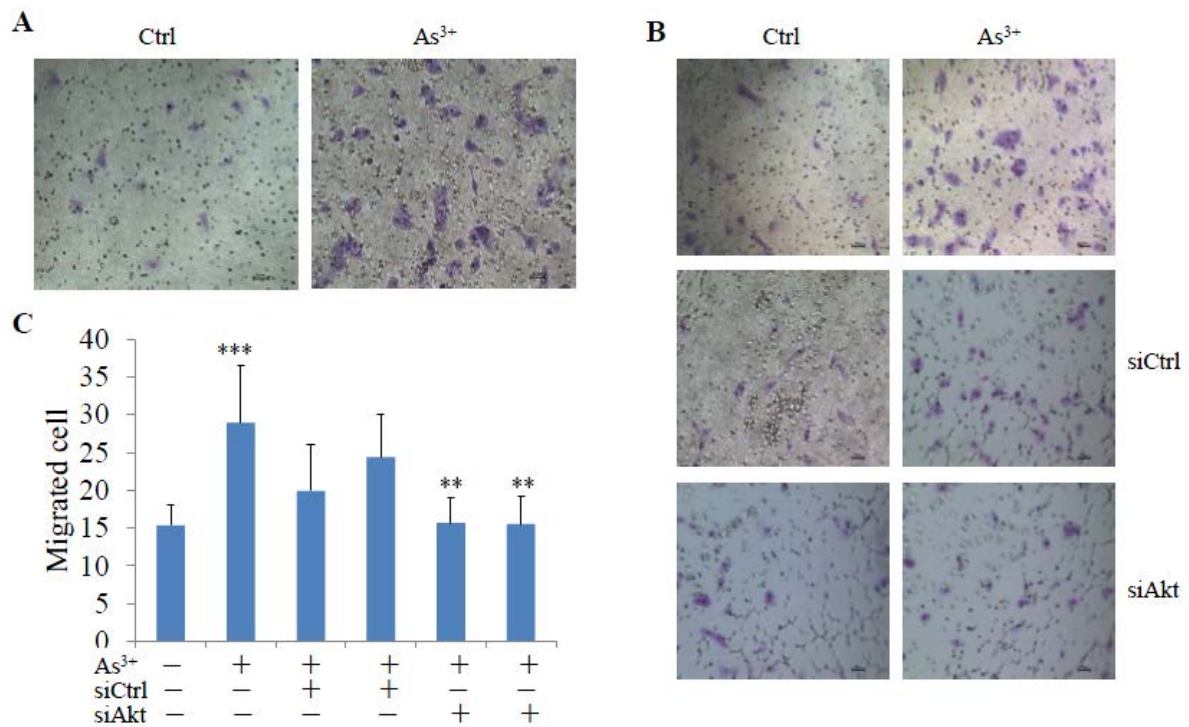
Figure 3.2.4 As³⁺-induced cell migration is Akt dependent.

(A), Migration assay shows elevated motility of the BEAS-2B cells treated with 20 µM As³⁺ for 24 h. (B), Silencing Akt by siRNA reduces As³⁺-induced cell migration. BEAS-2B cells were transfected with 50 nM control siRNA (siCtrl) or Akt siRNA (siAkt). (C), Semi-quantification of the migrated cells as shown in (B). Data are expressed as mean ± SD, n = 12, ***p < 0.001, **p < 0.01.
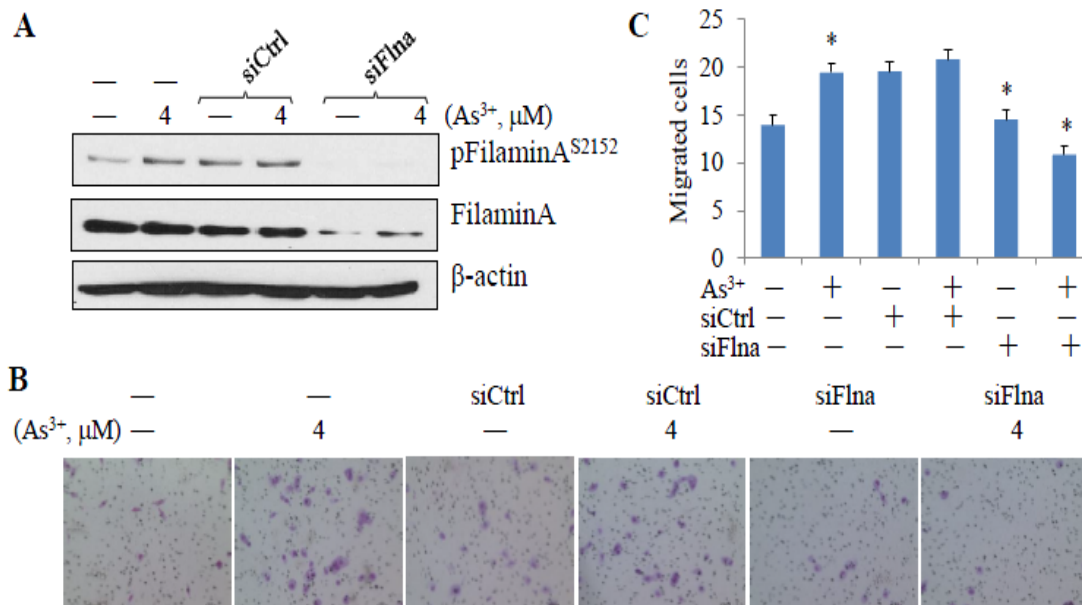
Figure 3.2.5 Silencing Filamin A prevented As^{3+}-induced cell migration.

(A), BEAS-2B cells were transfected with 50 nM control siRNA (siCtrl) or filamin

A siRNA (siFlna) with or without treatment by 4 µM As^{3+} for 24 h. (B),

Representative images of the migration assays. BEAS-2B cells were treated as

in (A). C. Semi-quantification of the migrated cells as shown in (B). Data are

expressed as mean ± SD, n = 12, *p < 0.05.

Several lines of evidence had indicated the essential role of filamin A for

mammalian cell locomotion. However, how this function of filamin A is regulated

remains to be fully understood. Since As^{3+} induces direct interaction between Akt

and filamin A (Fig. 3.2.2), which leads to S2152 phosphorylation of filamin A

(Figs. 3.2.3 A and B), it is likely that the migration regulation by filamin A depends

on the phosphorylation of filamin A at S2152. To explore this possibility, we

transfected BEAS-2B cells with an expression vector containing myc-tagged full-length filamin A (myc-Flna, wild-type) or myc-tagged filamin A in which the serine 2152 was mutated to alanine (S2152A). The substitution of S2152 with alanine abrogated the phosphorylation of filamin A as revealed in an IP experiment using anti-myc tag antibody (Fig. 3.2.6 A). Resembling the cells treated with As^{3+}, cells with an overexpression of the full-length wild-type filamin A exhibited an enhanced migration capability (Figs. 3.2.6 B and C). On the other hand, the migratory ability of the cells expressing the mutated filamin A, S2152A, was much reduced relative to the cells expressing wild-type filamin A (Figs. 3.2.5 B and C). Thus, phosphorylation of filamin A at S2152 by As^{3+}-activated Akt is a prerequisite step for cell migration.
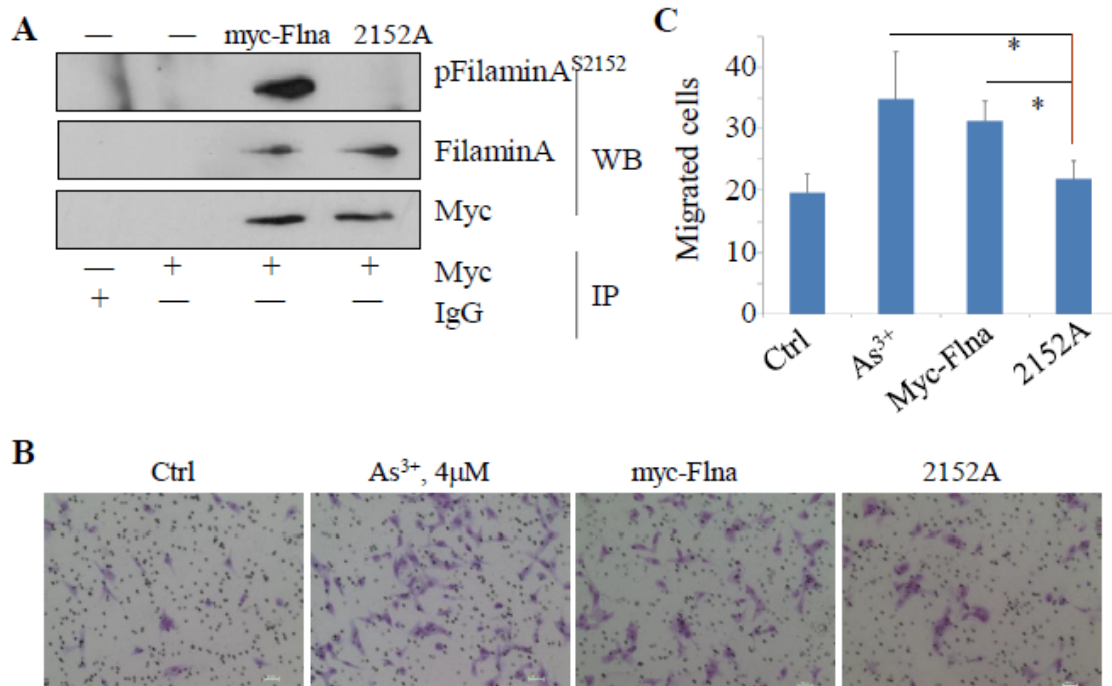
Figure 3.2.6 Phosphorylation of Filamin A on Ser2152 is required for As^{3+}-induced cell migration.

(A), BEAS-2B cells were transfected with 2 μg myc-filamin A (wild type, myc-Flna) plasmid or myc-filamin A S2152A (2152A) plasmid, followed by IP using anti-myc tag antibody and WB using the indicated antibodies. (B), Representative images of cell migration assay of the BEAS-2B cells that were transfected with 2 μg myc-filamin A (myc-Flna) plasmid or myc-filamin A S2152A (2152A) plasmid. (C), Semi-quantification of the migrated cells as shown in (A & B). Data are expressed as mean ± SD, n = 12, *p < 0.05.

To establish clinical relevance of the above findings, we investigated correlation between the expression level of filamin A and the survival times of the lung cancer patients by using an online database of Kaplan-Meier Plotter that

contains gene profiling information from 2,437 human lung cancer samples(Gyorffy, Surowiak et al. 2013). Three overlapping sets of probes are included in this database to mostly detect the open-reading-frame (ORF) of the filamin A mRNA. In initial analysis, we found that the expression level of filamin A did not distinguish poorer or better survival times of the patients when all types of lung cancers were included. After stratifying the lung cancer patients based on their status of cigarette smoking, e.g., never-smoked or smoked, it was found that higher expression level of filamin A predicts poorer overall survival of the patients who were never-smoked (Fig. 3.2.7 A). In contrast, higher expression of filamin A appeared to be no effect on the overall survival among those patients who were current or former smokers (Fig. 3.2.7 B). Since it had been well-documented that cigarette smoking contributes to different histological subtypes of the lung cancer(Tse, Mang et al. 2009), we believed that the opposite predictive power of filamin A expression between smoked and never-smoked might be a reflection of the different histological subtypes of the lung cancers. Therefore, we next compared the overall survival of the patients with either adenocarcinoma or squamous cell carcinoma based on the higher or lower expression level of filamin A. It is true that higher level of filamin A predicts a significant poorer survival of the patients with adenocarcinoma (Fig. 3.2.7 C), but not the squamous cell carcinoma (Fig. 3.2.7 D).
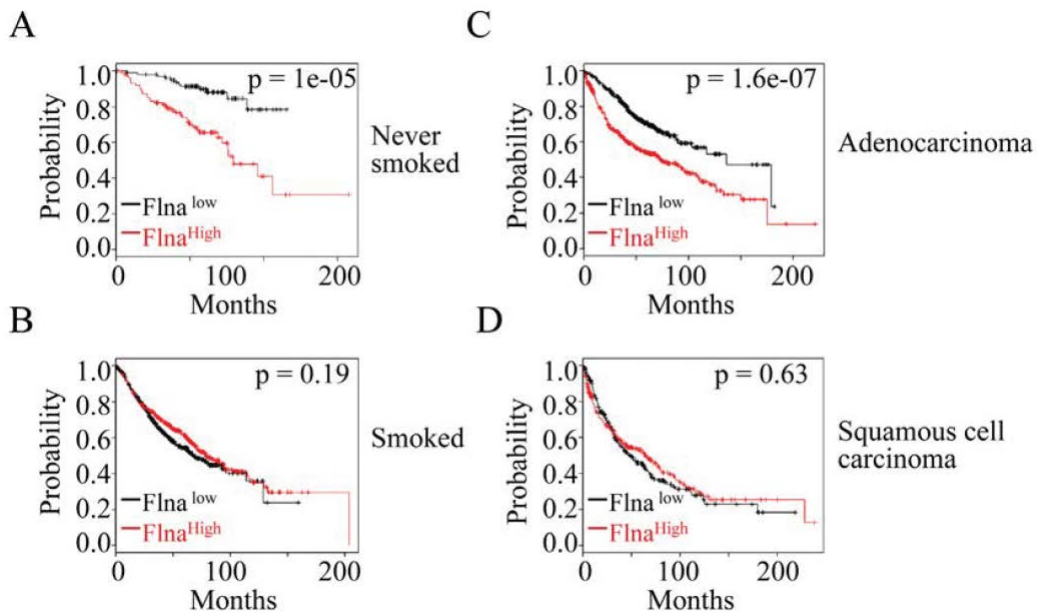
Figure3.2.7 The expression level of filamin A is a prognostic factor for the lung cancer patients.

A & B. High level of filamin A predicts poorer overall survival of the lung cancer patients who were never-smoked, but not those who were smoked. C & D. High level of filamin A predicts poorer overall survival of the patients with adenocarcinoma, but not those patients with squamous cell carcinoma. Statistical significance was determined by logrank *p*-values as indicated. The panels depict Kaplan-Meier survival probability with the probe ID 200859_x_at. Similar data were obtained when probe ID 214752_x_at and 2137

3.3 Discussion

The molecular or biochemical basis of As^{3+}-induced cell transformation, carcinogenesis and tumorigenesis is not well defined. In the present study, we identified a signaling cascade for As^{3+}-induced cell migration. In both human HEK-293 cells and bronchial epithelial cell line BEAS-2B cells, our data suggest that As^{3+} induces activation of Akt that interacts with and phosphorylates filamin A, an actin-binding protein responsible for crosslinking actin filaments into the membrane glycoproteins and integrins(Nakamura, Stossel et al. 2011, Wickstead and Gull 2011, Savoy and Ghosh 2013). Activation of Akt by As^{3+} appears to be ROS dependent, based on the fact that NAC, a widely used antioxidant, blocked As^{3+}-induced Akt activation and the subsequent filamin A phosphorylation. This notion was additionally supported by the observation that H_2O_2, the most common intracellular oxidative molecule, can activate Akt, leading to the phosphorylation of filamin A. Silencing either Akt or filamin A using specific siRNAs impaired cell migration in response to As^{3+}. Furthermore, our data also demonstrated that Akt-dependent phosphorylation on S2152 of filamin A is involved in cell migration, since overexpression of the mutated filamin A, in which S2152 was replaced with alanine, reduced the capability of cell migration. Taken together, these results provide the first evidence indicating that As^{3+} induces cell migration through signaling pathway from ROS to Akt that phosphorylates filamin A.

The association between environmental As^{3+} exposure and carcinogenesis had been well-established. Majority of studies so far addressed the potential effects of As^{3+} on the initiation of cell transformation and/or carcinogenesis, such as DNA damage responses, inhibition of the DNA repairing machinery, impairment of the immune surveillance system, alteration of the epigenetic modifications on the genome, and activation of a wide range of signaling pathways that linked to transcription factors and gene expression(Hubaux, Becker-Santos et al. 2013). Very limited information is available, however, on whether As^{3+} is also capable of regulating the key processes of tumorigenesis, including tumor cell motility, invasion and metastasis. Several reports as well as our previous studies had suggested that As^{3+} is a potent activator for the multi-functional protein kinase Akt that had been linked to tumor angiogenesis, tumor cell metastasis and metabolism(Beezhold, Liu et al. 2011, Liu, Chen et al. 2012, Carpenter and Jiang 2013, Chen, Liu et al. 2013, Li, Qiu et al. 2014, Sun, Yu et al. 2014). Accumulating evidence has suggested that Akt can not only provide the cells with growth advantages by eliciting proliferative or anti-apoptotic signals but also engage with motility of the cells through regulating actin tethering and stress fiber assembly(Xue and Hemmings 2013). Thus, it is very likely that in addition to the earlier events of carcinogenesis, As^{3+} can also participate in the tumorigenic process through Akt activation.

As revealed by IP using anti-Akt phospho-substrate antibody followed by proteomic analysis of the proteins in the immunocomplexes, we provide the first

evidence demonstrating a direct interaction between Akt and filamin A in cellular response to As^{3+}. This interaction results in phosphorylation of filamin A at S2152. Akt-dependent phosphorylation of filamin A at S2152 has been previously determined in prostate cancer cells and the IGF-1-treated MCF-7 cells(Wang, Kreisberg et al. 2007, Ravid, Chuderland et al. 2008). It is believed that this phosphorylation can prevent cleavage of filamin A and enhance its association with caveolin-1. Few studies also implied that S2152 phosphorylation of filamin A by other protein kinases, such as PAK1 or RSK, might be involved in the formation of membrane ruffling and lamellipodia extension, the necessary steps for cell migration and tumor cell metastasis(Vadlamudi, Li et al. 2002, Woo, Ohta et al. 2004). Furthermore, studies using molecular dynamics simulations unraveled that phosphorylation of filamin A at S2152 can facilitate integrin binding of filamin A by conformational changes that open the primary binding site of integrin on the Ig repeat 21 of filamin A(Chen, Kolahi et al. 2009). Thus, an Akt-dependent phosphorylation of filamin A induced by As^{3+} may enhance the capability of integrin binding of filamin A, and consequently, foster migration of the cells.

The observation that increased filamin A expression predicts poorer overall survival of the never-smoked patients and adenocarcinoma (Fig.3.2.7) provided compensatory supporting evidence suggesting involvement of filamin A in lung malignancy. More importantly, it is possible that this observation serves as a strong indication that this protein may impact the aggressiveness of the specific

histological subtypes of the human lung cancer. Many earlier studies had revealed that adenocarcinoma most likely occurred in the younger, never-smoked and females with a much aggressive disease progression(Bourke, Milstein et al. 1992, Green, Fortoul et al. 1993). It is also noteworthy that there is an increased proportion of adenocarcinoma among U.S. copper smelter workers who were exposed to As^{3+} through inhalation(Wicks, Archer et al. 1981). Due to the higher frequency of mutation on the gene loci encoding LKB1, an extensively studied tumor suppressor that suppresses metastasis of the tumor cells, adenocarcinoma appears to be more metastatic compared with squamous cell carcinoma or large cell carcinoma(Sanchez-Cespedes, Parrella et al. 2002, Ji, Ramsey et al. 2007). As tumor cell metastasis is one of the major biological factors contributing to the aggressiveness of tumors, it is plausible, thus, to assume that increased level of filamin A can enhance the migration and metastasis potentials of the cancer cells, especially for the adenocarcinoma. Although phosphorylation status of filamin A on patient prognostic outcomes was not evaluated due to the unavailability of such data, a proportional increase of the phosphorylated filamin A can be envisioned among those patients with a higher level of overall expression of filamin A. Accordingly, the prediction of poorer survival of the never-smoked lung cancer patients with adenocarcinoma is in great agreement with our experimental findings showing As^{3+} induces Akt-dependent phosphorylation of filamin A and cell migration.

In summary, this report presented a novel mechanism for the contributions of As^{3+} to human cancer. The data suggest that As^{3+} is capable of regulating the tumorigenesis through ROS dependent activation of protein kinase Akt that phosphorylates filamin A, leading to an enhanced crosslinking between actin filaments and integrin by filamin A and the subsequent migration of the cells. As cell motility or migration is one of the key steps for tumor cells metastasis (Moncharmont, Levy et al. 2014), regulation on the binding capability of filamin A on integrin and actin network certainly will influence the disease progression of the cancer patients. Indeed, a recent study showed that filamin A promotes migration and invasive potential of breast cancer cells through interaction with cyclin D1(Zhong, Yeow et al. 2010). This notion was further supported by the observations that overexpression of filamin A is associated with highly metastatic cancers, such as melanoma(Coughlin, Puig-de-Morales et al. 2006), neuroblastoma(Bachmann, Howard et al. 2006), breast cancer(Jiang, Yue et al. 2013), and prostate cancer(Bedolla, Wang et al. 2009). Accordingly, the findings in this report may be potentially translated into new therapeutic strategies by targeting Akt kinase and filamin A in cancers resulting from exposure to As^{3+} or other environmental carcinogens.

3.4 Materials and Methods

3.4.1 Cell lines and reagents -- The human bronchial epithelial cell line BEAS-2B, and human embryonic kidney 293 cell line HEK-293 were obtained from the American Type Culture Collection (ATCC, Manassas, VA). The BEAS-2B cells were cultured in Dulbecco's modified Eagle's medium (DMEM, Invitrogen, Grand Island, NY) containing 5% fetal bovine serum (FBS, Invitrogen), 1% penicillin/streptomycin, and 1% L-glutamine (Sigma, St. Louis, MO) at 37°C humidified incubator with 5% CO_2. The human embryonic kidney 293 cell line HEK-293 was maintained in DMEM containing 10% FBS, 1% penicillin/streptomycin, and 1% L-glutamine at 37°C humidified incubator with 5% CO_2. The cells were treated with As^{3+} [arsenic (III) chloride, Sigma-Aldrich, St. Louis, MO], with the indicated concentrations and times when the cells reached an approximately 80% confluence. In some experiments, PI3K/Akt inhibitor Wortmannin or ROS scavenger N-acetyl-cysteine (NAC) were added 2 h prior to As^{3+} treatment.

3.4.2 Plasmid preparation and transfection -- Constructs of pcDNA3-myc-Flna wild type (WT) and pcDNA3-myc-Flna S2152A were purchased from Addgene (Cambridge, MA). The plasmid DNA was amplified in DH5α Competent cells (Invitrogen, Grand Island, NY) and purified using either Plasmid Purification Kit (QIAGEN, Valencia, CA) or HQ Mini Plasmid Purification Kit (Invitrogen) according to the manufacturer's protocol. Cells in 6-well plates were transfected either with 50 ng plasmid DNA using Lipofectamine RNAiMAX Transfection

Reagent (Invitrogen) or 2 µg plasmid DNA with Nucleofector (Lonza, Anaheim, CA) with program G016.

3.4.3 Western Blotting -- For regular Western blotting, the cell lysates were prepared by RIPA cell lysis buffer (Cell Signaling, Danvers, MA) followed by ultrasonication and centrifugation. The supernatants were aspirated and proteins were quantified using a SpectraMax spectrophotometer (MDA Analytical Technologies). LDS sample buffer (Invitrogen) and dithiothreitol were added before denature. The samples were separated on 7.5% SDS-PAGE running gel and then transferred to PVDF membranes. The membranes were blocked in 5% non-fat milk in TBST and incubated with the indicated primary antibodies at 4°C overnight, and then incubated with second antibodies at room temperature for 1 h and washed with TBST 3 times for 10 min each. The protein levels were detected using CDP-Star Reagent (New England Biolabs, Ipswich, MA), SuperSignal West Pico (Thermo Fisher Scientific, Waltham, MA) or Immobilon Western chemiluminescent HRP substrate (MILLIPORE, Billerica, MA). The primary antibodies used in Western blotting include anti-phospho-Akt (Ser473) (Cell Signaling), anti-phospho-Akt substrate RXRXXS*/T* (Cell Signaling), anti-phospho-Filamin A (Cell Signaling), anti-Filmain A (Cell Signaling), anti-Akt (Cell Signaling), anti-myc tag, (Cell Signaling), anti-GAPDH (Cell Signaling), and anti-β-actin (Sigma).

3.4.4 SiRNA Transfection -- Cells with a concentration of 1×10^5/ml were seeded into 6-well plates and reverse transfected with siRNAs using

Lipofectamine RNAiMAX reagent (Invitrogen). For short term treatment, 20 µM As^{3+} was added at 24 h and cultured for an additional 2 h. SiRNA that specifically silence filamin A was purchased from Santa Cruz Technology (Santa Cruz, CA); control siRNA and siRNA specifically silencing Akt were purchased from Cell Signaling (Beverly, MA).

3.4.5 Immunoprecipitation (IP) and Proteomics -- After the indicated treatments, the cells were collected in IP lysis buffer and fragmented through passing the cells in a syringe equipped with 21.5 needle for 10–15 times. About 500 µg protein for each indicated sample was prepared and then incubated with the specific antibodies that were conjugated with agarose beads at 4°C agitation overnight. The immunocomplexes were pulled down by centrifugation at 3,000 rpm for 10 min and separated in SDS-PAGE gel for regular Western blotting. After extensive washes, the protein bands of interest on the PVDF membrane were retrieved with a scalpel followed by washing the membrane slices in double diluted water. Proteins on the membrane slices were digested overnight in 50 mM ammonium bicarbonate, 30% acetonitrile and sequencing-grade trypsin (Promega, Madison, WI) at 37°C. The digestion solution was collected and the membranes were washed 2 times with 70% acetonitrile (ACN) and 1% FA with sonication. The solutions were pooled, speed vacuumed to dryness, and solubilized in 2% ACN, 0.1% FA. Protein peptides were separated by reverse phase chromatography (Acclaim PepMap100C18 column, Thermo Scientific), followed by ionization with the Nanospray Flex Ion Source (Thermo Scientific),

and introduced into an orbitrap Fusion mass spectrometer (Thermo Scientific). The obtained spectra were analyzed using Proteome Discoverer 1.4.0.288 (Thermo Scientific) which incorporates the Mascot algorithm (Matrix Science, Boston, MA).

3.4.6 Cell Migration and Invasion Assay -- Cell migration was determined using BD BioCoat^{TM} Matrigel^{TM} Migration Chambers (8 μm filter). BEAS-2B cells were seeded with a density of 1.5×10^4/well (siRNA transfection) or 1×10^5 /well (plasmid transfection) in the upper chamber. DMEM medium containing 5% FBS was added into the lower chambers. The chambers were incubated at 37°C for 4 to 6 h, followed by replacing the medium contain 0.5% FBS and 4 μM As^{3+}. After 24 hrs incubation, the cells in the upper chambers were scrubbed out using cotton-tipped swab. The cells on the lower surface of the membrane were stained with the Diff-Quik Kit (Dade Behring). The migrated cells were counted under a microscope for 12 random fields in each group.

3.4.7 Statistics-- Microsoft Excel was used for statistical analyses of the quantitative data. The data are expressed as the mean ± standard deviation (SD), and Student's t-tests were used to determine the statistical significance of differences between samples treated under different conditions. Differences were considered statistically significant when *$p < 0.05$, **$p < 0.01$ or ***$p<0.005$.

REFERENCES

Akhavan-Niaki, H. and A. A. Samadani (2013). "DNA methylation and cancer development: molecular mechanism." Cell Biochem Biophys 67(2): 501-513.

Anetor, J. I., H. Wanibuchi and S. Fukushima (2007). "Arsenic exposure and its health effects and risk of cancer in developing countries: micronutrients as host defence." Asian Pac J Cancer Prev 8(1): 13-23.

Bachmann, A. S., J. P. Howard and C. W. Vogel (2006). "Actin-binding protein filamin A is displayed on the surface of human neuroblastoma cells." Cancer Sci 97(12): 1359-1365.

Bedolla, R. G., Y. Wang, A. Asuncion, K. Chamie, S. Siddiqui, M. M. Mudryj, T. J. Prihoda, J. Siddiqui, A. M. Chinnaiyan, R. Mehra, R. W. de Vere White and P. M. Ghosh (2009). "Nuclear versus cytoplasmic localization of filamin A in prostate cancer: immunohistochemical correlation with metastases." Clin Cancer Res 15(3): 788-796.

Beezhold, K., J. Liu, H. Kan, T. Meighan, V. Castranova, X. Shi and F. Chen (2011). "miR-190-mediated downregulation of PHLPP contributes to arsenic-induced Akt activation and carcinogenesis." Toxicol Sci 123(2): 411-420.

Beezhold, K. J., V. Castranova and F. Chen (2010). "Microprocessor of microRNAs: regulation and potential for therapeutic intervention." Mol Cancer 9: 134.

Bjerkvig, R., B. B. Tysnes, K. S. Aboody, J. Najbauer and A. J. Terzis (2005). "Opinion: the origin of the cancer stem cell: current controversies and new insights." <u>Nat Rev Cancer</u> **5**(11): 899-904.

Blejer, H. P. and W. Wagner (1976). "Inorganic arsenic--ambient level approach to the control of occupational cancerigenic exposures." <u>Ann N Y Acad Sci</u> **271**: 179-186.

Bourke, W., D. Milstein, R. Giura, M. Donghi, M. Luisetti, A. H. Rubin and L. J. Smith (1992). "Lung cancer in young adults." <u>Chest</u> **102**(6): 1723-1729.

Bower, J. J., S. S. Leonard, F. Chen and X. Shi (2006). "As(III) transcriptionally activates the gadd45a gene via the formation of H2O2." <u>Free Radic Biol Med</u> **41**(2): 285-294.

Cai, Z. and L. J. Yan (2013). "Protein Oxidative Modifications: Beneficial Roles in Disease and Health." <u>J Biochem Pharmacol Res</u> **1**(1): 15-26.

Calatayud, M., J. Gimeno, D. Velez, V. Devesa and R. Montoro (2010). "Characterization of the intestinal absorption of arsenate, monomethylarsonic acid, and dimethylarsinic acid using the Caco-2 cell line." <u>Chem Res Toxicol</u> **23**(3): 547-556.

Carpenter, R. L. and B. H. Jiang (2013). "Roles of EGFR, PI3K, AKT, and mTOR in heavy metal-induced cancer." <u>Curr Cancer Drug Targets</u> **13**(3): 252-266.

Chang, L. and M. Karin (2001). "Mammalian MAP kinase signalling cascades." <u>Nature</u> **410**(6824): 37-40.

Chang, Q., D. Bhatia, Y. Zhang, T. Meighan, V. Castranova, X. Shi and F. Chen (2007). "Incorporation of an internal ribosome entry site-dependent mechanism in arsenic-induced GADD45 alpha expression." Cancer Res **67**(13): 6146-6154.

Chang, Q., B. Chen, C. Thakur, Y. Lu and F. Chen (2014). "Arsenic-induced sub-lethal stress reprograms human bronchial epithelial cells to CD61 cancer stem cells." Oncotarget **5**(5): 1290-1303.

Chang, Q., J. Pan, X. Wang, Z. Zhang, F. Chen and X. Shi (2010). "Reduced reactive oxygen species-generating capacity contributes to the enhanced cell growth of arsenic-transformed epithelial cells." Cancer Res **70**(12): 5127-5135.

Chappell, S. A., J. P. LeQuesne, F. E. Paulin, M. L. deSchoolmeester, M. Stoneley, R. L. Soutar, S. H. Ralston, M. H. Helfrich and A. E. Willis (2000). "A mutation in the c-myc-IRES leads to enhanced internal ribosome entry in multiple myeloma: a novel mechanism of oncogene de-regulation." Oncogene **19**(38): 4437-4440.

Chen, B., J. Liu, Q. Chang, K. Beezhold, Y. Lu and F. Chen (2013). "JNK and STAT3 signaling pathways converge on Akt-mediated phosphorylation of EZH2 in bronchial epithelial cells induced by arsenic." Cell Cycle **12**(1): 112-121.

Chen, F. (2012). "JNK-induced apoptosis, compensatory growth, and cancer stem cells." Cancer Res **72**(2): 379-386.

Chen, F., L. M. Demers and X. Shi (2002). "Upstream signal transduction of NF-kappaB activation." Curr Drug Targets Inflamm Allergy **1**(2): 137-149.

Chen, F., M. Ding, V. Castranova and X. Shi (2001). "Carcinogenic metals and NF-kappaB activation." Mol Cell Biochem **222**(1-2): 159-171.

Chen, F., Y. Lu, Z. Zhang, V. Vallyathan, M. Ding, V. Castranova and X. Shi (2001). "Opposite effect of NF-kappa B and c-Jun N-terminal kinase on p53-independent GADD45 induction by arsenite." J Biol Chem **276**(14): 11414-11419.

Chen, F., Z. Zhang, J. Bower, Y. Lu, S. S. Leonard, M. Ding, V. Castranova, H. Piwnica-Worms and X. Shi (2002). "Arsenite-induced Cdc25C degradation is through the KEN-box and ubiquitin-proteasome pathway." Proc Natl Acad Sci U S A **99**(4): 1990-1995.

Chen, H. S., K. S. Kolahi and M. R. Mofrad (2009). "Phosphorylation facilitates the integrin binding of filamin under force." Biophys J **97**(12): 3095-3104.

Cheng, J. Q., C. W. Lindsley, G. Z. Cheng, H. Yang and S. V. Nicosia (2005). "The Akt/PKB pathway: molecular target for cancer drug discovery." Oncogene **24**(50): 7482-7492.

Chou, W. C. and C. V. Dang (2005). "Acute promyelocytic leukemia: recent advances in therapy and molecular basis of response to arsenic therapies." Curr Opin Hematol **12**(1): 1-6.

Chowdhury, R., R. Chatterjee, A. K. Giri, C. Mandal and K. Chaudhuri (2010). "Arsenic-induced cell proliferation is associated with enhanced ROS

generation, Erk signaling and CyclinA expression." <u>Toxicol Lett</u> **198**(2): 263-271.

Ciavardelli, D., C. Rossi, D. Barcaroli, S. Volpe, A. Consalvo, M. Zucchelli, A. De Cola, E. Scavo, R. Carollo, D. D'Agostino, F. Forli, S. D'Aguanno, M. Todaro, G. Stassi, C. Di Ilio, V. De Laurenzi and A. Urbani (2014). "Breast cancer stem cells rely on fermentative glycolysis and are sensitive to 2-deoxyglucose treatment." <u>Cell Death Dis</u> **5**: e1336.

Coughlin, M. F., M. Puig-de-Morales, P. Bursac, M. Mellema, E. Millet and J. J. Fredberg (2006). "Filamin-a and rheological properties of cultured melanoma cells." <u>Biophys J</u> **90**(6): 2199-2205.

Del Razo, L. M., B. Quintanilla-Vega, E. Brambila-Colombres, E. S. Calderon-Aranda, M. Manno and A. Albores (2001). "Stress proteins induced by arsenic." <u>Toxicol Appl Pharmacol</u> **177**(2): 132-148.

Dillon, R. L. and W. J. Muller (2010). "Distinct biological roles for the akt family in mammary tumor progression." <u>Cancer Res</u> **70**(11): 4260-4264.

Dong, Z. (2002). "The molecular mechanisms of arsenic-induced cell transformation and apoptosis." <u>Environ Health Perspect</u> **110 Suppl 5**: 757-759.

English, J., G. Pearson, J. Wilsbacher, J. Swantek, M. Karandikar, S. Xu and M. H. Cobb (1999). "New insights into the control of MAP kinase pathways." <u>Exp Cell Res</u> **253**(1): 255-270.

Fry, R. C., P. Navasumrit, C. Valiathan, J. P. Svensson, B. J. Hogan, M. Luo, S. Bhattacharya, K. Kandjanapa, S. Soontararuks, S. Nookabkaew, C. Mahidol, M. Ruchirawat and L. D. Samson (2007). "Activation of inflammation/NF-kappaB signaling in infants born to arsenic-exposed mothers." <u>PLoS Genet</u> **3**(11): e207.

Gebel, T. (2000). "Confounding variables in the environmental toxicology of arsenic." <u>Toxicology</u> **144**(1-3): 155-162.

Goldmann, W. H. (2002). "p56(lck) Controls phosphorylation of filamin (ABP-280) and regulates focal adhesion kinase (pp125(FAK))." <u>Cell Biol Int</u> **26**(6): 567-571.

Green, L. S., T. I. Fortoul, G. Ponciano, C. Robles and O. Rivero (1993). "Bronchogenic cancer in patients under 40 years old. The experience of a Latin American country." <u>Chest</u> **104**(5): 1477-1481.

Gyorffy, B., P. Surowiak, J. Budczies and A. Lanczky (2013). "Online survival analysis software to assess the prognostic value of biomarkers using transcriptomic data in non-small-cell lung cancer." <u>PLoS One</u> **8**(12): e82241.

Hammer, A., L. Rider, P. Oladimeji, L. Cook, Q. Li, R. R. Mattingly and M. Diakonova (2013). "Tyrosyl phosphorylated PAK1 regulates breast cancer cell motility in response to prolactin through filamin A." <u>Mol Endocrinol</u> **27**(3): 455-465.

Hanahan, D. and R. A. Weinberg (2011). "Hallmarks of cancer: the next generation." <u>Cell</u> **144**(5): 646-674.

He, H. J., S. Kole, Y. K. Kwon, M. T. Crow and M. Bernier (2003). "Interaction of filamin A with the insulin receptor alters insulin-dependent activation of the mitogen-activated protein kinase pathway." <u>J Biol Chem</u> **278**(29): 27096-27104.

Henkler, F., J. Brinkmann and A. Luch (2010). "The role of oxidative stress in carcinogenesis induced by metals and xenobiotics." <u>Cancers (Basel)</u> **2**(2): 376-396.

Hock, H. (2012). "A complex Polycomb issue: the two faces of EZH2 in cancer." <u>Genes Dev</u> **26**(8): 751-755.

Hu, Y., X. Jin and E. T. Snow (2002). "Effect of arsenic on transcription factor AP-1 and NF-kappaB DNA binding activity and related gene expression." <u>Toxicol Lett</u> **133**(1): 33-45.

Hubaux, R., D. D. Becker-Santos, K. S. Enfield, D. Rowbotham, S. Lam, W. L. Lam and V. D. Martinez (2013). "Molecular features in arsenic-induced lung tumors." <u>Mol Cancer</u> **12**: 20.

Jang, H., T. W. Kim, S. Yoon, S. Y. Choi, T. W. Kang, S. Y. Kim, Y. W. Kwon, E. J. Cho and H. D. Youn (2012). "O-GlcNAc regulates pluripotency and reprogramming by directly acting on core components of the pluripotency network." <u>Cell Stem Cell</u> **11**(1): 62-74.

Ji, H., M. R. Ramsey, D. N. Hayes, C. Fan, K. McNamara, P. Kozlowski, C. Torrice, M. C. Wu, T. Shimamura, S. A. Perera, M. C. Liang, D. Cai, G. N. Naumov, L. Bao, C. M. Contreras, D. Li, L. Chen, J. Krishnamurthy, J.

Koivunen, L. R. Chirieac, R. F. Padera, R. T. Bronson, N. I. Lindeman, D. C. Christiani, X. Lin, G. I. Shapiro, P. A. Janne, B. E. Johnson, M. Meyerson, D. J. Kwiatkowski, D. H. Castrillon, N. Bardeesy, N. E. Sharpless and K. K. Wong (2007). "LKB1 modulates lung cancer differentiation and metastasis." Nature **448**(7155): 807-810.

Jiang, B. H. and L. Z. Liu (2009). "PI3K/PTEN signaling in angiogenesis and tumorigenesis." Adv Cancer Res **102**: 19-65.

Jiang, R., Y. Li, A. Zhang, B. Wang, Y. Xu, W. Xu, Y. Zhao, F. Luo and Q. Liu (2014). "The acquisition of cancer stem cell-like properties and neoplastic transformation of human keratinocytes induced by arsenite involves epigenetic silencing of let-7c via Ras/NF-kappaB." Toxicol Lett **227**(2): 91-98.

Jiang, X., J. Yue, H. Lu, N. Campbell, Q. Yang, S. Lan, B. G. Haffty, C. Yuan and Z. Shen (2013). "Inhibition of filamin-A reduces cancer metastatic potential." Int J Biol Sci **9**(1): 67-77.

Joseph, T., B. Dubey and E. A. McBean (2015). "Human health risk assessment from arsenic exposures in Bangladesh." Sci Total Environ **527-528**: 552-560.

Kapahi, P., T. Takahashi, G. Natoli, S. R. Adams, Y. Chen, R. Y. Tsien and M. Karin (2000). "Inhibition of NF-kappa B activation by arsenite through reaction with a critical cysteine in the activation loop of Ikappa B kinase." J Biol Chem **275**(46): 36062-36066.

Karin, M. (2008). "The IkappaB kinase - a bridge between inflammation and cancer." Cell Res **18**(3): 334-342.

Kelly, K. and U. Siebenlist (1985). "The role of c-myc in the proliferation of normal and neoplastic cells." J Clin Immunol **5**(2): 65-77.

Kim, E., M. Kim, D. H. Woo, Y. Shin, J. Shin, N. Chang, Y. T. Oh, H. Kim, J. Rheey, I. Nakano, C. Lee, K. M. Joo, J. N. Rich, D. H. Nam and J. Lee (2013). "Phosphorylation of EZH2 activates STAT3 signaling via STAT3 methylation and promotes tumorigenicity of glioblastoma stem-like cells." Cancer Cell **23**(6): 839-852.

Komar, A. A. and M. Hatzoglou (2011). "Cellular IRES-mediated translation: the war of ITAFs in pathophysiological states." Cell Cycle **10**(2): 229-240.

Kozak, M. (2005). "A second look at cellular mRNA sequences said to function as internal ribosome entry sites." Nucleic Acids Res **33**(20): 6593-6602.

Kuninty, P. R., L. Bojmar, V. Tjomsland, M. Larsson, G. Storm, A. Ostman, P. Sandstrom and J. Prakash (2016). "MicroRNA-199a and -214 as potential therapeutic targets in pancreatic stellate cells in pancreatic tumor." Oncotarget **7**(13): 16396-16408.

Lemaitre, J. M., R. S. Buckle and M. Mechali (1996). "c-Myc in the control of cell proliferation and embryonic development." Adv Cancer Res **70**: 95-144.

Li, G., L. S. Lee, M. Li, S. W. Tsao and J. F. Chiu (2011). "Molecular changes during arsenic-induced cell transformation." J Cell Physiol **226**(12): 3225-3232.

Li, L., Y. Lu, P. M. Stemmer and F. Chen (2015). "Filamin A phosphorylation by Akt promotes cell migration in response to arsenic." Oncotarget **6**(14): 12009-12019.

Li, L., P. Qiu, B. Chen, Y. Lu, K. Wu, C. Thakur, Q. Chang, J. Sun and F. Chen (2014). "Reactive oxygen species contribute to arsenic-induced EZH2 phosphorylation in human bronchial epithelial cells and lung cancer cells." Toxicol Appl Pharmacol **276**(3): 165-170.

Li, M., J. F. Cai and J. F. Chiu (2002). "Arsenic induces oxidative stress and activates stress gene expressions in cultured lung epithelial cells." J Cell Biochem **87**(1): 29-38.

Li, Q., M. M. Harraz, W. Zhou, L. N. Zhang, W. Ding, Y. Zhang, T. Eggleston, C. Yeaman, B. Banfi and J. F. Engelhardt (2006). "Nox2 and Rac1 regulate H2O2-dependent recruitment of TRAF6 to endosomal interleukin-1 receptor complexes." Mol Cell Biol **26**(1): 140-154.

Li, X. H., K. C. McGrath, V. H. Tran, Y. M. Li, C. C. Duke, B. D. Roufogalis and A. K. Heather (2013). "Attenuation of Proinflammatory Responses by S-[6]-Gingerol via Inhibition of ROS/NF-Kappa B/COX2 Activation in HuH7 Cells." Evid Based Complement Alternat Med **2013**: 146142.

Liu, F. and K. Y. Jan (2000). "DNA damage in arsenite- and cadmium-treated bovine aortic endothelial cells." Free Radic Biol Med **28**(1): 55-63.

Liu, J., B. Chen, Y. Lu, Y. Guan and F. Chen (2012). "JNK-dependent Stat3 phosphorylation contributes to Akt activation in response to arsenic exposure." Toxicol Sci **129**(2): 363-371.

Liu, Z., E. Boles and B. P. Rosen (2004). "Arsenic trioxide uptake by hexose permeases in Saccharomyces cerevisiae." J Biol Chem **279**(17): 17312-17318.

Liu, Z., J. M. Carbrey, P. Agre and B. P. Rosen (2004). "Arsenic trioxide uptake by human and rat aquaglyceroporins." Biochem Biophys Res Commun **316**(4): 1178-1185.

Manning, B. D. and L. C. Cantley (2007). "AKT/PKB signaling: navigating downstream." Cell **129**(7): 1261-1274.

Margueron, R., G. Li, K. Sarma, A. Blais, J. Zavadil, C. L. Woodcock, B. D. Dynlacht and D. Reinberg (2008). "Ezh1 and Ezh2 maintain repressive chromatin through different mechanisms." Mol Cell **32**(4): 503-518.

Meo, S. A. and T. Al-Khlaiwi (2003). "Health hazards of welding fumes." Saudi Med J **24**(11): 1176-1182.

Moncharmont, C., A. Levy, J. B. Guy, A. T. Falk, M. Guilbert, J. C. Trone, G. Alphonse, M. Gilormini, D. Ardail, R. A. Toillon, C. Rodriguez-Lafrasse and N. Magne (2014). "Radiation-enhanced cell migration/invasion process: a review." Crit Rev Oncol Hematol **92**(2): 133-142.

Nakamura, F., T. P. Stossel and J. H. Hartwig (2011). "The filamins: organizers of cell structure and function." Cell Adh Migr **5**(2): 160-169.

Namgung, U. and Z. Xia (2001). "Arsenic induces apoptosis in rat cerebellar neurons via activation of JNK3 and p38 MAP kinases." Toxicol Appl Pharmacol **174**(2): 130-138.

Nguyen, H. L., S. Zucker, K. Zarrabi, P. Kadam, C. Schmidt and J. Cao (2011). "Oxidative stress and prostate cancer progression are elicited by membrane-type 1 matrix metalloproteinase." Mol Cancer Res **9**(10): 1305-1318.

Nishikawa, T., H. Wanibuchi, M. Ogawa, A. Kinoshita, K. Morimura, T. Hiroi, Y. Funae, H. Kishida, D. Nakae and S. Fukushima (2002). "Promoting effects of monomethylarsonic acid, dimethylarsinic acid and trimethylarsine oxide on induction of rat liver preneoplastic glutathione S-transferase placental form positive foci: a possible reactive oxygen species mechanism." Int J Cancer **100**(2): 136-139.

Pena, E., G. Arderiu and L. Badimon (2012). "Subcellular localization of tissue factor and human coronary artery smooth muscle cell migration." J Thromb Haemost **10**(11): 2373-2382.

Prasad, S., S. C. Gupta and A. K. Tyagi (2017). "Reactive oxygen species (ROS) and cancer: Role of antioxidative nutraceuticals." Cancer Lett **387**: 95-105.

Ramos, A., C. Santos, L. Alvarez, R. Nogues and M. P. Aluja (2009). "Human mitochondrial DNA complete amplification and sequencing: a new validated primer set that prevents nuclear DNA sequences of mitochondrial origin co-amplification." Electrophoresis **30**(9): 1587-1593.

Ravid, D., D. Chuderland, L. Landsman, Y. Lavie, R. Reich and M. Liscovitch (2008). "Filamin A is a novel caveolin-1-dependent target in IGF-I-stimulated cancer cell migration." Exp Cell Res **314**(15): 2762-2773.

Rognoni, L., J. Stigler, B. Pelz, J. Ylanne and M. Rief (2012). "Dynamic force sensing of filamin revealed in single-molecule experiments." Proc Natl Acad Sci U S A **109**(48): 19679-19684.

Roy, R. V., Y. O. Son, P. Pratheeshkumar, L. Wang, J. A. Hitron, S. P. Divya, R. D, D. Kim, Y. Yin, Z. Zhang and X. Shi (2015). "Epigenetic targets of arsenic: emphasis on epigenetic modifications during carcinogenesis." J Environ Pathol Toxicol Oncol **34**(1): 63-84.

Sanchez-Cespedes, M., P. Parrella, M. Esteller, S. Nomoto, B. Trink, J. M. Engles, W. H. Westra, J. G. Herman and D. Sidransky (2002). "Inactivation of LKB1/STK11 is a common event in adenocarcinomas of the lung." Cancer Res **62**(13): 3659-3662.

Sato, A., M. Okada, K. Shibuya, E. Watanabe, S. Seino, Y. Narita, S. Shibui, T. Kayama and C. Kitanaka (2014). "Pivotal role for ROS activation of p38 MAPK in the control of differentiation and tumor-initiating capacity of glioma-initiating cells." Stem Cell Res **12**(1): 119-131.

Savoy, R. M. and P. M. Ghosh (2013). "The dual role of filamin A in cancer: can't live with (too much of) it, can't live without it." Endocr Relat Cancer **20**(6): R341-356.

Shen, Y. A., C. Y. Wang, Y. T. Hsieh, Y. J. Chen and Y. H. Wei (2015). "Metabolic reprogramming orchestrates cancer stem cell properties in nasopharyngeal carcinoma." Cell Cycle **14**(1): 86-98.

Shi, Y., A. Sharma, H. Wu, A. Lichtenstein and J. Gera (2005). "Cyclin D1 and c-myc internal ribosome entry site (IRES)-dependent translation is regulated by AKT activity and enhanced by rapamycin through a p38 MAPK- and ERK-dependent pathway." J Biol Chem **280**(12): 10964-10973.

Shukla, V., T. Vaissiere and Z. Herceg (2008). "Histone acetylation and chromatin signature in stem cell identity and cancer." Mutat Res **637**(1-2): 1-15.

Singh, R., B. S. Shankar and K. B. Sainis (2014). "TGF-beta1-ROS-ATM-CREB signaling axis in macrophage mediated migration of human breast cancer MCF7 cells." Cell Signal **26**(7): 1604-1615.

Stoneley, M., F. E. Paulin, J. P. Le Quesne, S. A. Chappell and A. E. Willis (1998). "C-Myc 5' untranslated region contains an internal ribosome entry segment." Oncogene **16**(3): 423-428.

Sun, J., M. Yu, Y. Lu, C. Thakur, B. Chen, P. Qiu, H. Zhao and F. Chen (2014). "Carcinogenic metalloid arsenic induces expression of mdig oncogene through JNK and STAT3 activation." Cancer Lett **346**(2): 257-263.

Tokar, E. J., L. Benbrahim-Tallaa, J. M. Ward, R. Lunn, R. L. Sams, 2nd and M. P. Waalkes (2010). "Cancer in experimental animals exposed to arsenic and arsenic compounds." Crit Rev Toxicol **40**(10): 912-927.

Tse, L. A., O. W. Mang, I. T. Yu, F. Wu, J. S. Au and S. C. Law (2009). "Cigarette smoking and changing trends of lung cancer incidence by histological subtype among Chinese male population." Lung Cancer **66**(1): 22-27.

Vadlamudi, R. K., F. Li, L. Adam, D. Nguyen, Y. Ohta, T. P. Stossel and R. Kumar (2002). "Filamin is essential in actin cytoskeletal assembly mediated by p21-activated kinase 1." Nat Cell Biol **4**(9): 681-690.

Wang, R., M. Xin, Y. Li, P. Zhang and M. Zhang (2016). "The Functions of Histone Modification Enzymes in Cancer." Curr Protein Pept Sci **17**(5): 438-445.

Wang, Y., J. I. Kreisberg, R. G. Bedolla, M. Mikhailova, R. W. deVere White and P. M. Ghosh (2007). "A 90 kDa fragment of filamin A promotes Casodex-induced growth inhibition in Casodex-resistant androgen receptor positive C4-2 prostate cancer cells." Oncogene **26**(41): 6061-6070.

Wanibuchi, H., T. Hori, V. Meenakshi, T. Ichihara, S. Yamamoto, Y. Yano, S. Otani, D. Nakae, Y. Konishi and S. Fukushima (1997). "Promotion of rat hepatocarcinogenesis by dimethylarsinic acid: association with elevated ornithine decarboxylase activity and formation of 8-hydroxydeoxyguanosine in the liver." Jpn J Cancer Res **88**(12): 1149-1154.

Wanibuchi, H., E. I. Salim, A. Kinoshita, J. Shen, M. Wei, K. Morimura, K. Yoshida, K. Kuroda, G. Endo and S. Fukushima (2004). "Understanding arsenic carcinogenicity by the use of animal models." Toxicol Appl Pharmacol **198**(3): 366-376.

Watanabe, T., T. Sato, T. Amano, Y. Kawamura, N. Kawamura, H. Kawaguchi, N. Yamashita, H. Kurihara and T. Nakaoka (2008). "Dnm3os, a non-coding RNA, is required for normal growth and skeletal development in mice." Dev Dyn **237**(12): 3738-3748.

Wicks, M. J., V. E. Archer, O. Auerbach and M. Kuschner (1981). "Arsenic exposure in a copper smelter as related to histological type of lung cancer." Am J Ind Med **2**(1): 25-31.

Wickstead, B. and K. Gull (2011). "The evolution of the cytoskeleton." J Cell Biol **194**(4): 513-525.

Woo, M. S., Y. Ohta, I. Rabinovitz, T. P. Stossel and J. Blenis (2004). "Ribosomal S6 kinase (RSK) regulates phosphorylation of filamin A on an important regulatory site." Mol Cell Biol **24**(7): 3025-3035.

Wu, W. S., J. R. Wu and C. T. Hu (2008). "Signal cross talks for sustained MAPK activation and cell migration: the potential role of reactive oxygen species." Cancer Metastasis Rev **27**(2): 303-314.

Xu, X., S. Duan, F. Yi, A. Ocampo, G. H. Liu and J. C. Izpisua Belmonte (2013). "Mitochondrial regulation in pluripotent stem cells." Cell Metab **18**(3): 325-332.

Xue, G. and B. A. Hemmings (2013). "PKB/Akt-dependent regulation of cell motility." J Natl Cancer Inst **105**(6): 393-404.

Xue, G., D. F. Restuccia, Q. Lan, D. Hynx, S. Dirnhofer, D. Hess, C. Ruegg and B. A. Hemmings (2012). "Akt/PKB-mediated phosphorylation of Twist1

promotes tumor metastasis via mediating cross-talk between PI3K/Akt and TGF-beta signaling axes." <u>Cancer Discov</u> **2**(3): 248-259.

Yin, G., R. Chen, A. B. Alvero, H. H. Fu, J. Holmberg, C. Glackin, T. Rutherford and G. Mor (2010). "TWISTing stemness, inflammation and proliferation of epithelial ovarian cancer cells through MIR199A2/214." <u>Oncogene</u> **29**(24): 3545-3553.

Yu, M., J. Sun, C. Thakur, B. Chen, Y. Lu, H. Zhao and F. Chen (2014). "Paradoxical roles of mineral dust induced gene on cell proliferation and migration/invasion." <u>PLoS One</u> **9**(2): e87998.

Zhang, Y., D. Bhatia, H. Xia, V. Castranova, X. Shi and F. Chen (2006). "Nucleolin links to arsenic-induced stabilization of GADD45alpha mRNA." <u>Nucleic Acids Res</u> **34**(2): 485-495.

Zheng, C. Y., S. K. Lam, Y. Y. Li and J. C. Ho (2015). "Arsenic trioxide-induced cytotoxicity in small cell lung cancer via altered redox homeostasis and mitochondrial integrity." <u>Int J Oncol</u> **46**(3): 1067-1078.

Zhong, J., D. Lardinois, J. Szilard, M. Tamm and M. Roth (2011). "Rat mesothelioma cell proliferation requires p38delta mitogen activated protein kinase and C/EBP-alpha." <u>Lung Cancer</u> **73**(2): 166-170.

Zhong, Z., W. S. Yeow, C. Zou, R. Wassell, C. Wang, R. G. Pestell, J. N. Quong and A. A. Quong (2010). "Cyclin D1/cyclin-dependent kinase 4 interacts with filamin A and affects the migration and invasion potential of breast cancer cells." <u>Cancer Res</u> **70**(5): 2105-2114.

ABSTRACT

UNDERLYING MECHANISMS OF ARSENIC-INDUCED TUMORIGENESIS:

FROM EPIGENETICS TO MALIGNANCY

by

LINGZHI LI

August 2017

Advisor: Dr. Fei Chen

Major: Pharmaceutical Sciences

Degree: Doctor of Philosophy

Arsenic is a well-recognized environmental health threat with the capability of inducing a number of human diseases, including cancer. The aim of this dissertation is to unveil the mechanisms underlying the carcinogenic activities of environmental arsenic. The biological functions of arsenic had been studied for decades. However, there are still many questions that remain to be fully answered, such as whether and how arsenic contributes to the epigenetic regulations and migration or metastasis control of the cancer cells. In this regard, we focused our attention on both histone modifications and miRNA regulations in the arsenic-induced malignant transformation of the cells, and tried to establish the signaling cascades that mediate arsenic-induced transformation. Furthermore, we investigated the downstream functional pathways related to malignancy through biochemical and proteomics analyses. Based on the results from the first specific aim, we had demonstrated that long term treatment of the cells with

arsenic at concentrations that are comparable to environment arsenic exposure is able to induce EZH2 phosphorylation that facilitates its cytoplasmic localization, and the expression of c-myc. Meanwhile, we also noted that long-term treatment of the cells with arsenic induces expression of miR-214 and miR-199a along with a metabolic reprogramming of the cells from mitochondrial oxidative phosphorylation to cytoplasmic glycolysis (Warburg Effects). In the second specific aim, we further identified interaction of mdig and Filamin A phosphorylation that is involved in cell motility and migration induced by arsenic. Collectively, our studies on the novel pathways induced by arsenic provide new insights for the carcinogenetic mechanism of arsenic and shed light on the prevention and promising therapeutic strategies for human cancers that are associated with environmental arsenic exposure.

AUTOBIOGRAPHICAL STATEMENT

LINGZHI LI

EDUCATION
B.S. Biological Engineering, Shenyang Pharmaceutical University (SPU)
09/2008- 07/2012
Ph. D. Pharmaceutical Sciences, Wayne State University (WSU) 09/2012-now

HONORS & AWARDS
Thomas C. Rumble Fellowship, Wayne State University, 08/2015-08/2016
Best Poster Award in the 9th Conference on Metal Toxicity & Carcinogenesis,
10/2016

PUBLICATIONS
1. Li, L. and F. Chen (2017). "Arsenic and SUMO wrestling in protein modification." Cell Cycle: 1-2.
2. Li, L. and F. Chen (2016). "Oxidative stress, epigenetics, and cancer stem cells in arsenic carcinogenesis and prevention." Curr Pharmacol Rep 2(2): 57-63.
3. Li, L., Y Lu, Stemmer PM, Chen F. (2015). Filamin A phosphorylation by Akt promotes cell migration in response to arsenic. Oncotarget 2015, 5:12009-12019.
4. Li, L., P. Qiu, Chen B, Lu Y, Wu K, Thakur C, Chang Q, Sun J, Chen F. Reactive oxygen species contribute to arsenic-induced EZH2 phosphorylation in human bronchial epithelial cells and lung cancer cells. Toxicol Appl Pharmacol 2014, 276(3):165-170.
5. Wu, K., L. Li, Thakur, C., Lu, Y., Zhang, X., Yi, Z., Chen, F. et al. (2016). "Proteomic Characterization of the World Trade Center dust-activated mdig and c-myc signaling circuit linked to multiple myeloma." Sci Rep 6: 36305.
6. Wu, K., Q. Chang, Lu Y, Qiu P, Chen B, Thakur C, Sun J, Li, L., Kowluru A, Chen F. Gefitinib resistance resulted from STAT3-mediated Akt activation in lung cancer cells." Oncotarget 2013, 4(12): 2430-2438.

POSTER PRESENTATIONS
Lingzhi Li, Yongju Lu, Fei Chen. Arsenic-induced reactive oxygen species in Akt activation and cell migration. 8th Conference on Metal Toxicity and Carcinogenesis, University of New Mexico, October 26, 2014

Lingzhi Li, Kai Wu, Yongju Lu, Chitra Thakur, Fei Chen. Increased miR214/199a renders the metabolic shift through mitochondrial inhibition during arsenic-induced malignant transformation. 9th Annual Conference on Metal Toxicity & Carcinogenesis, University of Kentucky, October 16-19, 2016